CHLAMYDIA TRACHOMATIS CAUSES CHROMOSOME SEGREGATION ERRORS LEADING TO CYTOKINESIS FAILURE

By

HEATHER MARIE BROWN

A DISSERTATION PRESENTED TO THE GRADUATE SCHOOL
OF THE UNIVERSITY OF FLORIDA IN PARTIAL FULFILLMENT
OF THE REQUIREMENTS FOR THE DEGREE OF
DOCTOR OF PHILOSOPHY

UNIVERSITY OF FLORIDA

2013

To Granddad, for always being one of my biggest fans

ACKNOWLEDGMENTS

I would like to thank my parents for their love and unending support. I would have not made it through my PhD without my mom coming to keep me company and cook me delicious meals when I had an awful week and my dad reminding me to take it one day at a time. I would like to thank my brothers, Erik and Alex, for being protective and my partner in crime.

I would like to thank my mentor Dr. Scott Grieshaber for your amazing patience. I know it took a lot of work to get me from only being able to take pictures on the microscope to being able to change a mercury bulb and trouble shoot all the crazy things people do to our scope.

I would also like to thank my committee members Dr. Edward Chan, Dr. Paul Gulig, Dr. Brian Law, and Dr. Daniel Purich. Thank you for taking your time out of your schedule to meet with me and give helpful advice. I was sad when I was told my third aim was boring, but in the end it really strengthened my project.

Next, I would like to thank Dr. Nicole Grieshaber and Dr. Shannon Wallet for all their great advice and help. It's wonderful to have auxiliary mentors for extra support.

Finally I would like to thank the lab, I wouldn't have made it through the program, without having a group to commit shenanigans with. Specifically, without Andrea I might have quit and become a zookeeper. Instead, I'm now an expert on *Chlamydia.*

TABLE OF CONTENTS

page

LIST OF TABLES

LIST OF FIGURES

LIST OF ABBREVIATIONS

APC	anaphase promoting complex
CCV	*Coxiella* containing vacuole
CDK1	cyclin-dependent kinase-1
CPAF	chlamydial protease-like activity factor
DNA	deoxyribonucleic acid
EB	elementary body
FISH	Fluorescence *in situ* hydrization
FUCCI	fluorescence ubiquitination cell cycle indicator
G	*Chlamydia trachomatis* serovar G
G1	gap phase
G2	second gap phase
GAPDH	glyceraldehyde 3-phosphate dehydrogenase
GFP	green fluorescent protein
GPIC	*Chlamydia caviae* (Guinea Pig Infective Conjunctivitis)
HBSS	Hank's Balanced Salt Solution
HPV	human papillomavirus
IRA	International Research Agency
IFU	inclusion forming unit
KDA	kilodalton
L2	*Chlamydia trachomatis* serovar L2
M	molar
MOI	multiplicity of infection
MOPN	*Chlamydia muridarum* (Mouse pneumonitis)

MTOC	microtubule organizing center
NMBD	nuclear membrane breakdown
NuMA	nuclear mitotic apparatus protein
PBS	phosphate buffered saline
PCM	pericentriolar material
PCR	polymerase chain reaction
RB	reticulate body
RFP	red fluorescent protein
S	synthesis phase
SAC	spindle assembly checkpoint
SEM	standard error of the mean
STI	sexually transmitted infection
TARP	translocated actin-recruiting phosphoprotein
UV	ultraviolet

Abstract of Dissertation Presented to the Graduate School
of the University of Florida in Partial Fulfillment of the
Requirements for the Degree of Doctor of Philosophy

CHLAMYDIA TRACHOMATIS CAUSES CHROMOSOME SEGREGATION ERRORS LEADING TO CYTOKINESIS FAILURE

By

Heather Marie Brown

May 2013

Chair: Scott S. Grieshaber
Major: Medical Sciences - Immunology and Microbiology

Chlamydiae are obligate intracellular bacteria that cause a variety of diseases in both humans and animals. Infection with *Chlamydia trachomatis* can lead to host cell multinucleation. Our goal was to determine the mechanism by which a chlamydial infection leads to cytokinesis failure. We demonstrated that cytokinesis failure is not due to steric interference and through live cell imaging showed that cytokinesis failure occurs at abscission. Cells that failed in cytokinesis contained DNA in the midbody of the dividing cell. Therefore we investigated changes in mitosis. Infected cells have a reduced mitotic index, suggesting that infected cells spend less time in mitosis, which allows less time to organize chromosomes. Furthermore, we demonstrated that *C. trachomatis* infected cells are able to escape a monastrol block, suggesting a premature exit from mitosis. We conclude that *C. trachomatis* induce a premature exit from mitosis that causes DNA in the midbody of the cell, resulting in cytokinesis failure at abscission.

Next, we investigated if cytological changes were conserved among chlamydial species. *C. trachomatis* L2 causes shortened mitosis, declustering of amplified centrosomes and cytokinesis failure resulting in multinucleation. We compared *C. trachomatis* to *Chlamydia muridarum* and *Chlamydia caviae* to determine the

conservation of these effects between different *Chlamydia* species. All three species were able to cause a decrease in mitotic index and amplified centrosomes. We observed a greater percentage of multinucleated cells and multipolar spindles due to *C. trachomatis* infection compared to the other *Chlamydia* species. The spindle multipolarity was the only cytological change that followed the observed trend in multinucleation. We found that spindle multipolarity correlated to centrosome displacement and spread during interphase in infected cells. These results suggest that Chlamydia species may interact differently with host centrosomes, resulting in varying rates of multinucleation. We hypothesize that different cytological changes among species correlate with the ability to cause transformation.

CHAPTER 1
INTRODUCTION

Chlamydia

Chlamydiae are gram-negative obligate intracellular bacteria that require the entry into mucosal epithelial cells to grow and replicate (Swanson et al., 1975; Moulder, 1991). *Chlamydia* consists of a large group of species that have the ability to infect organisms as diverse as amoebas and mammals (Wheelhouse and Longbottom, 2012). Different disease etiologies can occur depending on the serovar, even within the same species. The ocular serovars of the human pathogen *Chlamydia trachomatis* cause trachoma, the leading cause of infectious blindness worldwide (Burton and Mabey, 2009). The urogenital serovars are the causative agent of chlamydia, the most commonly reported STI worldwide with an estimated 92 million new cases annually (WHO, 2001). Genital infections are often subclinical and therefore left untreated, allowing the infection to become chronic. Chronic infections can lead to serious health sequelae such as pelvic inflammatory disease and tubal infertility in untreated women (Cates and Wasserheit, 1991). *Chlamydia* has also been clinically associated with cytologic cervical atypia (Kiviat et al., 1985) and epidemiologically linked to an increase in the risk for cervical cancer (Anttila et al., 2001; Smith et al., 2002; Madeleine et al., 2007). A direct molecular mechanism responsible for this link has yet to be described.

Chlamydiae undergo a unique biphasic developmental cycle. During the developmental cycle *Chlamydia* alternates between two distinct forms, the elementary body (EB) and the reticulate body (RB). The EB is the small (0.3 μm), non-replicating, infectious form, while the RB is the large (1.0 μm), metabolically active form (Friis, 1972; Moulder, 1991). The infection begins with the EBs interacting with the host cell

membrane through electrostatic interactions. The EB then induces phagocytosis by the type three secretion system injecting the effector TARP (translocated actin-recruiting phosphoprotein) into the host cell, promoting actin remodeling and uptake (Clifton et al., 2004). Upon entry into the host cell, the EB quickly differentiates to the reticulate body (RB). While inside the host cell, *Chlamydia* resides within a vacuole termed an inclusion, which grows during the course of infection. RBs replicate until an unknown signal causes the RBs to differentiate back to EBs asynchronously (Friis, 1972). Some RBs continue to replicate to produce RBs and EBs until lysis. The EBs are released and disseminate to initiate another round of infection (Moulder, 1991).

The inclusion formed by *Chlamydia* allows it to reside within a privileged niche inside the host cell. *Chlamydia* alters the properties of the inclusion shortly after entry by insertion of proteins into the inclusion membrane. These membrane modifications ensure that the inclusion is not acidified by fusion with the endocytic or lysosomal pathway (Fields and Hackstadt, 2002). To increase in size and acquire nutrients, the inclusion intercepts sphingomyelin and cholesterol from the exocytic pathway (Hackstadt et al., 1995; Saka and Valdivia, 2010).

Chlamydial proteins on the inclusion interact with microtubules in a dynein-dependent and dynamitin-independent fashion (Grieshaber et al., 2003). The chlamydial inclusion migrates along microtubules to the microtubule-organizing center (MTOC). Migration to the MOTC is conserved among chlamydial species suggesting that MOTC localization is critical for the developmental cycle of *Chlamydia*. The inclusion remains in close association with the MTOC throughout the host cell cycle and remains physically attached to centrosomes during mitosis (Grieshaber et al., 2006).

The obligate intracellular nature of the chlamydial infectious life cycle requires *Chlamydia* to reprogram many aspects of cellular function to render the cell hospitable to growth. Chlamydiae have a type III secretion system (T3SS) as well as an uncharacterized type II-dependent secretion system. These secretion systems secrete protein effectors into the host cell, modulating cellular behavior to create its unique intracellular niche (Zhong, 2011). One class of proteins that is translocated by the T3SS is the Inc proteins (Inclusion membrane proteins), which comprise 7-10% of the proteome (Dehoux et al., 2011). The Inc proteins are inserted into the inclusion membrane and are characterized by a unique bilobal hydrophobic domain. Many of these Inc proteins also contain predicted coiled coil domains that suggest that Inc proteins interact with host proteins (Dehoux et al., 2011). Although Inc proteins are found in all *Chlamydiae*, specific Inc proteins are not well conserved (Read et al., 2000).

Another way that *Chlamydia* manipulates its environment is through protease activity altering host protein levels. *Chlamydia* encodes approximately two dozen proteins with proteolytic activity (Stephens et al., 1998; Zhong, 2011). The most well studied chlamydial protease is the chlamydial protease-like activity factor (CPAF), which is translocated to the host cytoplasm (Zhong et al., 2001; Shaw et al., 2002). CPAF is first translated as a proenzyme. Maturation occurs with dimerization and self-proteolysis, which regulates activity (Dong et al., 2004). Although true CPAF substrates are currently in question, CPAF is necessary for growth of *Chlamydia* and the inclusion (Jorgensen et al., 2011; Chen et al., 2012).

Chlamydia infection induces a variety of cytopathic effects such as centrosome amplification, degradation of host proteins and multinucleation of the host cell (Greene

and Zhong, 2003; Grieshaber et al., 2006; Paschen et al., 2008; Johnson et al., 2009). Each of these defects can contribute to aneuploidy and chromosome instability in mammals (Chan, 2011; Weihua et al., 2011).

Host Cell

Chlamydial infection of dividing cells causes a number of significant changes to the cellular pathways controlling cell division. Infection causes disorganized spindle assembly, early mitotic exit and amplification of centrosomes during G2 of the cell cycle (Johnson et al., 2009; Knowlton et al., 2011). Maintenance of cell cycle control is critical for normal cell division and is therefore a heavily regulated process

Effects on the Cell Cycle

To replicate, the cell undergoes a series of events termed a cell cycle. The eukaryotic cell cycle is divided into two periods: interphase, when the cell grows in size, and mitosis, the period when the cell divides the nuclear material. Interphase is further divided into three stages: Gap 1 (G_1), Synthesis (S), and Gap 2 (G_2) (Figure 1-1). G_1 allows cells to determine if there are adequate nutrients available to begin the cell cycle (Menoyo et al., 2013). Furthermore, during G_1 a cell determines if DNA damage has occurred during mitosis. If DNA damage has occurred, cells are delayed in G_1 so that the damage can be repaired before entry to S phase (Clémenson and Marsolier-Kergoat, 2009). S phase is the portion of the cell cycle when chromosomes are replicated so the two forming daughter cells will receive identical complements of chromosomes. After S phase, the cell progresses into G_2. During G_2 the cell grows in size and again monitors for DNA damage (Clémenson and Marsolier-Kergoat, 2009). If the cell is free of DNA damage, it will enter mitosis.

Chromosomes are physically divided during mitosis. This process is tightly regulated to ensure that a symmetrical division occurs, allowing daughter cells to inherit the proper complement of chromosomes. Mitosis is divided into five stages: prophase, prometaphase, metaphase, anaphase and telophase (Figure 1-1). Prophase is characterized by chromosome condensation and nuclear envelope breakdown. Prophase is followed by prometaphase during which the chromosomes are pushed and pulled by the microtubules of the mitotic spindle until aligned in the center of the cell (Wandke et al., 2012). The cell has entered metaphase once the chromosomes align in the center of the cell, termed the metaphase plate. Once chromosomes are aligned along the metaphase plate, the protein complex cohesin is cleaved allowing for sister chromosomes to separate and enter anaphase (Uhlmann et al., 1999). Mitosis concludes with telophase in which the nuclear envelope reforms and chromosomes decondense.

The cell cycle undergoes a unidirectional sequence due to a class of proteins termed cyclins whose levels rise and fall causing progression through the phases. (Benanti, 2012). Cyclin expression is controlled through both transcriptional regulation and ubiquitin-targeted proteasome degradation. Their function is to bind and activate cyclin-dependent kinases (Cdks) whose activity is required for the cell to pass through the phases of the cell cycle (Pines, 2011). In order to enter S-phase, Cyclin D1 must be expressed to activate Cdk4/6 (Jirawatnotai et al., 2012). Similarly, to enter mitosis Cyclin B1 binds and activates Cdk1, which facilitates nuclear envelope breakdown and chromosome condensation (Gavet and Pines, 2010).

Mitotic exit is controlled by the Spindle Assembly Checkpoint, which ensures that exit only occurs when a symmetrical mitotic spindle has formed. To satisfy the Spindle Assembly Checkpoint, all of the kinetochores must be attached to the mitotic spindle microtubules (Hartwell and Weinert, 1989). Once the checkpoint is satisfied the Anaphase Promoting Complex (APC) ubiquitinates securin and Cyclin B1, targeting them for degradation by the proteasome. Securin degradation releases its binding partner, separase. Separase is a protease that degrades cohesin, the protein structure that forms a ring around sister chromosomes (Peters, 2006). This cascade allows sister chromosomes to separate and the cell to proceed to anaphase. When Cyclin B1 is degraded, it inactivates its binding partner cyclin dependent kinase 1 (Cdk1). Inactivation of Cdk1 allows phosphatases to dephosphorylate targets of Cdk1 causing the cell to exit mitosis and reform the nuclear envelope (Baker et al., 2007).

In order for the mitosis to result in two new daughter cells, the cell must undergo cytokinesis. Cytokinesis is the process of physically separating two cells. Cytokinesis begins during anaphase when the cell positions the actin-myosin contractile ring at the metaphase plate. The actin-myosin ring contracts to form a cleavage furrow followed by an intercellular bridge. The intercellular bridge is a 1 μm cytoplasmic connection between postmitotic sister cells (Steigemann and Gerlich, 2009b). The intercellular bridge contains tightly compacted microtubules and hundreds of proteins involved in the cytoskeleton, membrane traffic and signaling (Eggert et al., 2006). The intercellular bridge is very protein-dense and causes a barrier for diffusion between the two cells (Schmidt and Nichols, 2004). At the center of the intercellular bridge is a structure termed the midbody. The midbody is the area where antiparallel microtubules overlap

and are covered in an electron-dense matrix (Steigemann and Gerlich, 2009b). This structure provides an anchor for the ingressed cleavage furrow. The final step of cytokinesis is abscission, which is characterized by the resolution of the membrane between the postmitotic daughter cells (Glotzer, 2001; 2005). Both postmitotic daughter cells traffic exocytosed membrane to the midbody of the cell. Resolution of the intracellular bridge occurs when proteins have been cleared of the abscission point and new membrane has been delivered.

Abscission cannot be reversed; therefore, a final checkpoint controls this crucial step. The NoCut pathway monitors for DNA in the midbody of the dividing cell, which occur due to DNA segregation errors. (Norden et al., 2006) Upon activation, the NoCut pathway pauses the cell in cytokinesis to allow DNA an opportunity to be removed out of the midbody. DNA removal is important to prevent irreversible damage that would occur during abscission. If the DNA is not removed from the midbody, the cell will undergo cleavage furrow regression and abort cytokinesis resulting in a multinucleated cell (Mendoza et al., 2009).

The prevailing hypothesis for the fate of tetraploid cells is that they arrest in G_1 due to p53 and the arrest results in apoptosis or senescence of the cell (Andreassen et al., 2001). Recently, it has been found that some tetraploid cells with intact p53 continue to undergo the cell cycle suggesting that multinucleated cells are in fact viable (Uetake and Sluder, 2004).

Tetraploid cells can lead to aneuploidy by two mechanisms: chromosome aberrations and extra centrosomes (Fujiwara et al., 2005; Fukasawa, 2007; Ganem and Pellman, 2007). It is unclear how tetraploid cells accumulate chromosomal breaks and

rearrangements, but one possibility is damage through a chaotic mitosis causing physical force on the chromosome. DNA damage is further promoted by extra centrosomes when they are not clustered into a pseudo-bipolar spindle (Ganem and Pellman, 2012). Finally, extra centrosomes promote missegregation of chromosomes by creating asymmetrical forces that act upon chromosomes.

Effects on the Centrosome Cycle

Centrosomes are non-membranous organelles that form the microtubule organizing center (MTOC) which resides in a juxtanuclear position in eukaryotic cells (Gould and Borisy, 1977). A centrosome is composed of a mother and a daughter centriole that are crucial in anchoring microtubules and controlling the reproduction of centrosomes (Piel et al., 2000; Nigg, 2002). Each centriole is composed of nine sets of triplet microtubules, and a centrosome is composed of two sister centrioles. Sister centrioles are arranged orthogonally and are surrounded by an electron-dense cloud of proteins termed the pericentriolar material (PCM) (Vogel et al., 1997). The PCM contains over 200 proteins, which creates a scaffolding and a nucleation site for microtubules (Andersen et al., 2003). In normal animal cells there are one to two centrosomes present depending on the phase of the cell cycle (Figure 1-2). The cell undergoes a centrosome cycle to replicate the centrosome for mitosis. The centrosome cycle begins with untethering of the mother and daughter centrioles during anaphase (Kuriyama and Borisy, 1981). Separase, the same protease necessary for separation of sister chromatids, cleaves cohesin on sister centrioles and causes untethering (Schöckel et al., 2011). Upon entry into S-phase, the centrioles begin semi-conservative replication with growth of new centrioles on the proximal part of the existing centriole (Kuriyama and Borisy, 1981). During G2 the centrosomes mature and

recruit additional PCM. Finally, the two centrosomes separate through removal of the tether at mitotic entry, and the centrosome cycle begins again (Zyss and Gergely, 2009).

The centrosome cycle and the cell cycle are tightly coupled to ensure there are only two centrosomes when the cell enters mitosis. Tight coupling is accomplished by using the same machinery to regulate both the cell cycle and the centrosome cycle. One way they are coupled is by the activation of cyclin dependent kinase Cdk2 that is necessary for both DNA replication and centrosome duplication, successfully preparing the cell for mitosis (Ferguson and Maller, 2010).

Centrosome amplification occurs if the centrosome cycle is disturbed, the cell fails in cytokinesis, or fuses with another cell (Anderhub et al., 2012). In order to protect the cell from multipolar mitosis, eukaryotic cells have the innate ability to cluster extra centrosomes during interphase and mitosis (Ring et al, 1982). If centrosome clustering is disrupted, it can promote cellular transformation.

Cancer Biology

Since the 1990s it has been recognized that infectious agents contribute to a substantial portion of cancers worldwide. Pisani et al. proposed 15.6% of cancers in 1990 were caused by viruses, bacteria or parasites (Pisani et al., 1997). More recently, de Martel et al. performed a study in which they took into account only infectious agents that the International Agency of Research (IAR) had classified as carcinogenic. This study found the burden to be 16.1% or around two million of the cancer cases in 2008 could be attributed to infectious agents (de Martel et al., 2012). Studies such as these do not take into account infectious agents that are considered cofactors, such as HIV, so the contribution of infection may be underestimated.

Studies have linked *Chlamydia* as a cofactor for increased cancer rates due to prior infection (Koskela et al., 2000; Anttila et al., 2001; Smith et al., 2002; Matsumoto et al., 2003; Smith et al., 2004; Madeleine et al., 2007; Roset Bahmanyar et al., 2012). Studies performed by Koskela et al. 2000 and Anttila et al. 2001 compared serum samples of 530,000 Nordic women who were either diagnosed with cervical cancer or the matched control. These studies demonstrated that patients who were seropositive for *Chlamydia trachomatis* had a twofold increased risk for squamous cell carcinoma (Koskela et al., 2000; Anttila et al., 2001). A case study carried out by Smith et al. demonstrated that women seropositive for *C. trachomatis* and DNA-positive for HPV had a twofold increase in squamous cervical cancer, confirming previous studies (Smith et al., 2002). Additional studies have used chlamydial DNA as a marker for past infections and have had similar results. Wallen et al. 2002 performed a population-based study that examined samples from 130,000 women over a 26 year span. This study demonstrated a prior *C. trachomatis* infection was associated with an increased risk for the development of invasive cervical cancer (Wallin et al., 2002). Currently, the mechanism of how *Chlamydia* may contribute to cervical cancer is unknown.

One hundred years ago, Theodor Boveri first proposed that malignancies might be a result of abnormal mitosis due to extra centrosomes (Boveri, 2008). His hypothesis was widely ignored after the discovery of genes and somatic mutations. Recently, due to the observation that most solid tumors have supernumerary centrosomes, interest in the role of centrosome abnormalities in cellular transformation has increased (Brinkley and Goepfert, 1998; Pihan et al., 1998).

Although supernumerary centrosomes contribute to spindle multipolarity, extra centrosomes alone are insufficient. Eukaryotic cells are able to suppress the effects of extra centrosomes in order to undergo bipolar mitoses (Ring et al., 1982; Brinkley, 2001; Quintyne et al., 2005). Many cells that undergo a multipolar mitosis instead of bipolar mitosis are inviable due to substantial chromosome loss (Ganem et al., 2009). There are two ways that cells suppress the effects of amplified centrosomes to prevent multipolar spindles. The first is to functionally silence extra centrosomes preventing them from forming a spindle pole. Alternatively, cells have the ability to cluster extra centrosomes into two functional spindle poles (Nigg, 2002). Silencing and clustering extra centrosomes are not mutually exclusive and work together to transition from a multipolar spindle in prometaphase to a pseudo-bipolar spindle in anaphase, allowing for viable daughter cells (Thompson et al, 2010).

We have demonstrated that *Chlamydia* induces cytokinesis failure of the host cell. In the following chapters, we examine the effects chlamydial infection has on mitosis and centrosomes. We present evidence that the ability of *Chlamydia trachomatis* to override the Spindle Assembly Checkpoint, amplify centrosomes and decluster supernumerary centrosomes, causes DNA bridging and results in cytokinesis failure. All three phenotypes are necessary for inducing cytokinesis failure; higher rates of declustered centrosomes in chlamydial species correlate to higher rates of multinucleation. We propose a model in which *Chlamydia* causes cellular transformation through induction of chromosomal instability.

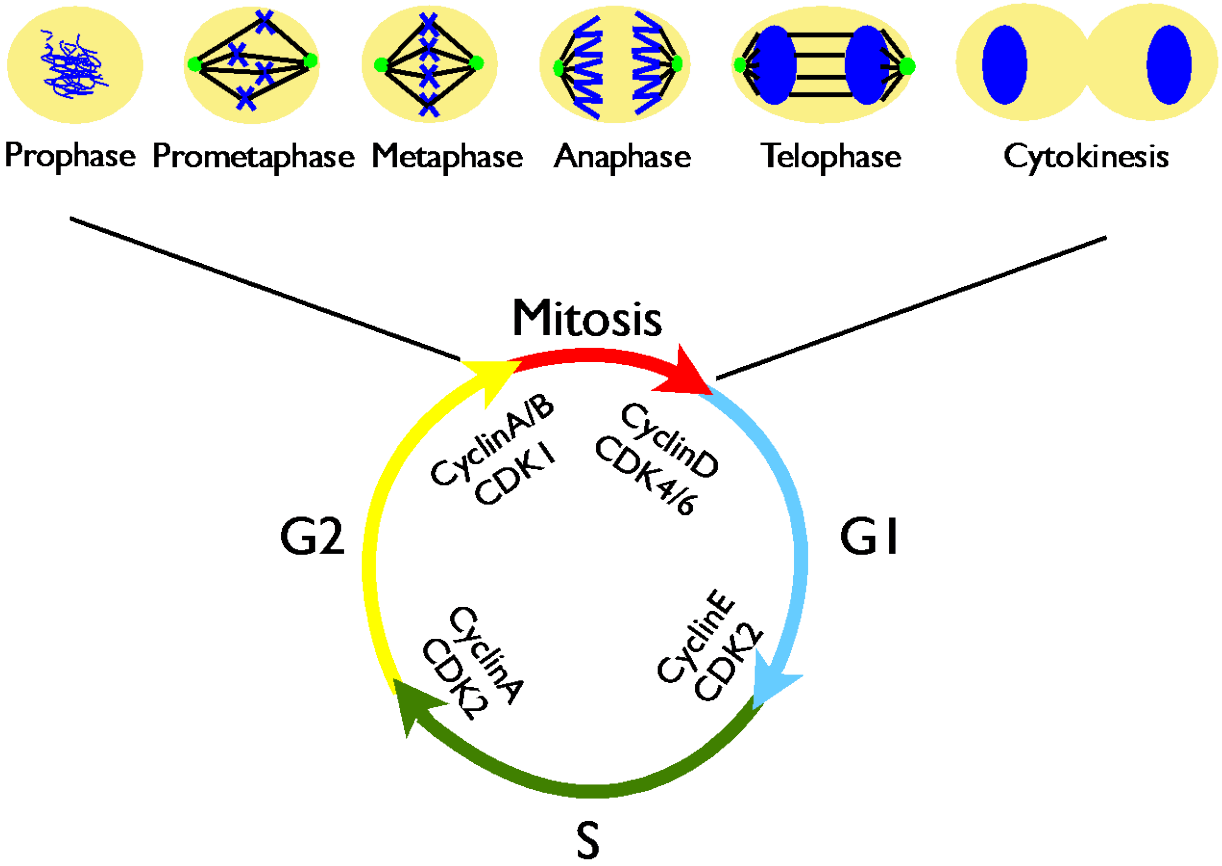

Figure 1-1. The cell cycle. The eukaryotic cell cycle is divided into two periods: interphase, when the cell grows in size, and mitosis, the period when the cell divides the nuclear material. Interphase is further divided into three stages: Gap 1 (G_1), Synthesis (S), and Gap 2 (G_2). Mitosis is divided into five phases: prophase, prometaphase, metaphase, anaphase and telophase. The cyclins important for progressing through the cell cycle are noted on the inside of the cell cycle.

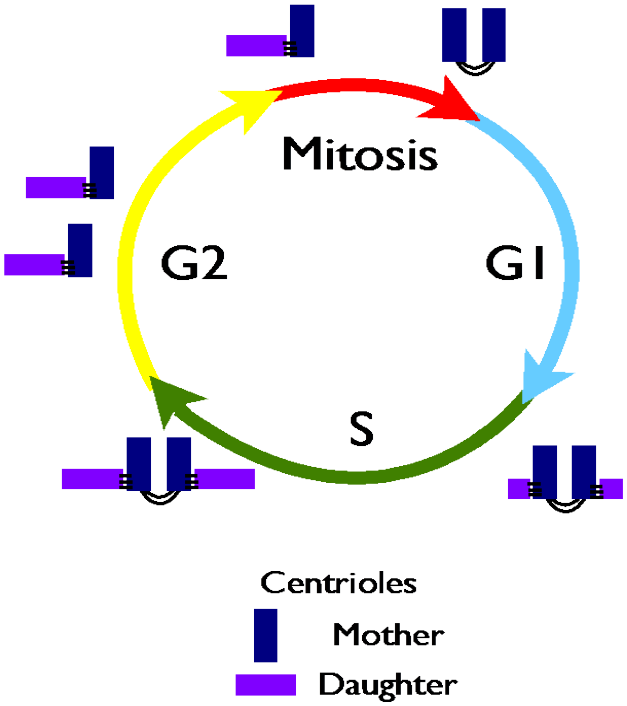

Figure 1-2. Centrosome Cycle. The centrosome cycle is a series of events that the cell undergoes in order to replicate centrosomes. Replication events coincide with replication events in the cell cycle. New centrioles form orthogonally to existing centrioles during S-phase. The two centrosomes disengage during G2 in order to create two spindle poles during mitosis.

CHAPTER 2
MATERIALS AND METHODS

Organisms and Cell Culture

Chlamydia trachomatis serovar L2 (LGV 434), *C. muriduram* Nigg strain (referred to as MoPn), and *C. caviae* GPIC (gift from Ted Hackstadt) were grown in McCoy cells, and EBs were purified by Renografin density gradient centrifugation as previously described (Caldwell et al., 1981). *Coxiella burnetii* Nine Mile phase II (NMII) clone 4 was a gift from Robert Heinzen, Rocky Mountain Labs, NIAID/NIH.

All cell lines were obtained from the American Type Culture Collection. HeLa 229 cells and Neuroblastoma (N1E-115) cells were grown in RPMI-1640 (Cellgro) supplemented with 10% fetal bovine serum (FBS) and 10 µg/ml gentamicin. BJ Human Foreskin Fibroblasts and McCoy cells were grown in DMEM (Cellgro) supplemented with 10% FBS and 10 µg/ml gentamicin.

Infections

Cells were incubated with *C. trachomatis*, *C. muridarum* or *C. caviae* EBs at an MOI of approximately 3 in Hank's balanced salt solution (HBSS) (Gibco) for 45 minutes at room temperature while rocking. The inoculum was removed and replaced with fresh RPMI-1640 containing 10% FBS and 10µg/ml gentamicin. For *C. burnetii* infections, the same procedure was used except the incubation was for 4 hours and no gentamicin was used.

Immunohistochemistry

Cells for fluorescent microscopy were grown on 12-mm number 1.5 borosilicate glass coverslips coated with Poly-L-lysine (Sigma). For antibody staining, the coverslips were fixed in ice-cold methanol for 10 minutes and incubated with the primary antibody

described for each experiment. The antibodies used for these experiments were: mouse monoclonal anti-β-tubulin (Sigma), mouse monoclonal anti-ɣ-tubulin (Sigma) and AlexaFluor 488 phalloidin (Invitrogen). *C. trachomatis* and *C. burnetii* were stained with platelet-poor human serum (Sigma). To visualize the primary antibodies, AlexaFluor 488-conjugated secondary antibodies against mouse IgG were used (Molecular Probes/Invitrogen). The far-red fluorescent DNA dye DRAQ5 (Biostatus) or Hoechst was used to visualize nuclei. Images were acquired using a spinning disk confocal system connected to a Leica DMIRB microscope with a 63x oil-immersion objective, equipped with a Photometrics cascade-cooled EMCCD camera, under the control of the Open Source software package μManager (http://micro-manager.org). Images where processed with image analysis software ImageJ (http://rsb.info.nih.gov/ij/). Images displayed for figures are maximal intensity projections of the 3D data sets, adjusted for brightness and contrast.

Transfections and Plasmids

HeLa cells were seeded on 25-mm number 1.5 glass coverslips in 6-well plates and grown to 70% confluency. Transfections were carried out using Lipofectamine 2000 (Invitrogen) according to the manufacturer's instructions. A stable cell line of RFP-H2B HeLa cells was selected with 5 μg/ml blasticidin (Fisher), and expression from the GFP vector was allowed to proceed for 48 hours to permit time for expression. Human H2B was cloned from pBOS-H2BGFP (BD Biosciences) into a RFP-destination vector using the Gateway Cloning System (Invitrogen) according to the manufacturer's instruction. Similarly, Bicaudal D1 was cloned from pOTB7-Bicaudal (ATCC) into a GFP-destination vector using the Gateway Cloning System.

Live Cell Imaging

Cells were transferred into high glucose DMEM media with 25 mM HEPES. The coverslip was overlayed with mineral oil, and the chamber was supplemented with CO_2. Images where acquired as previously described.

Cell Fusion Assay

HeLa cells were pre-stained with CytoTracker Red CMTPX or Green CMFDA (Molecular Probes) using recommended protocol. Both populations of cells were infected with *Chlamydia trachomatis* at an MOI of 3. The two populations of cells were seeded together on 25-mm number 1.5 glass coverslips in 6-well plates for 6 hpi. Cells were fixed with cold methanol at 30 hpi and stained with Draq5. Alternatively, cells were pre-stained and seeded without infection. The cells were then electroporated at 175V, 0Ω , 975 µF. Cells were imaged, and orange multinucleated cells were counted as positive for cell fusion.

Inclusion Measurement

HeLa cells were imaged using confocal microscopy. ImageJ was used to measure the area of the inclusion or CCV. We calculated and compared the 2 dimensional areas occupied by the CCV and inclusion to simplify quantification. In both the *Coxiella* CCV and chlamydial inclusion the Z component was comparable and did not significantly change over time. The flat cell shape highly constrained the shape of the vacuoles in the Z dimension, and significant growth only occurs in the X and Y dimensions.

Cell-Free Degradation Assay

Mitotic cell proteins were obtained through a mitotic shake-off of HeLa cells in Phosphate Buffered Saline (PBS). Cells were pelleted and resuspended in 0.5 mL of

NP-40 Buffer (1% NP-40, 150 mM NaCl, 0.5% Triton X-100 in 50 mM Tris pH 8) Protease inhibitor cocktail (Sigma) was added. Extraction was carried out on ice for 20 minutes and then centrifuged to pellet the debris. Supernatant was collected and kept at -80°Cuntil use. Chlamydial proteins were collected through harvesting the cytosolic fraction of cells infected with C. trachomatis serovar L2. Cells were scraped and centrifuged to form a pellet. Cells were resuspended in a douncing buffer (10mM KCl, 1.5mM MgCl2, 1mM EDTA, 1mM DTT, 250mM sucrose in 20mM Hepes-KOH pH 7.5). Cells were dounced, and the supernatants were harvested with a series of centrifugations with the final centrifugation at 100,000x g. CPAF peptide inhibitor (GenScript) was also added. For the degradation assay, mitotic host proteins and chlamydial cytosolic proteins were mixed and incubated for 1 hour at 37˚C.

Mitotic Index Assays

The mitotic index was calculated by determining the ratio of mitotic cells to the total number of cells present. For the infected populations, only infected cells were counted. A minimum of 1500 cells were counted over 20-30 fields, and the procedure was repeated three times. The SAC was induced with the kinesin-5 inhibitor monastrol (Sigma), and the mitotic index was again calculated. Cells were treated with monastrol at a final concentration of 100μM for a total of 36 hours. The cells were methanol fixed and stained with anti-β-tubulin to visualize monopolar spindle formation, DRAQ5, and anti-L2 antibodies where appropriate.

Western Blot

Proteins from the cell-free degradation assay were separated by SDS-polyacrylamide gels and transferred to nitrocellulose membranes. The primary antibodies were: mouse monoclonal anti-cyclin B1, rabbit polyclonal anti-cdc2, rabbit

polyclonal anti-cdc2 (Thr161), (Cell Signaling Technology), rabbit polyclonal anti-PTTG-1 (Invitrogen), mouse monoclonal anti-GAPDH (EnCor). Proteins were visualized with either goat anti-mouse perioxidase conjugated secondary antibodies (Thermo) or goat anti-rabbit perioxidase conjugated secondary antibodies (Sigma) and SuperSignal West Dura Extended Duration Substrate (Thermo).

Double Thymidine Block

HeLa cells where grown in 2mM thymidine in RPMI for 18 hours. Cells were then switched to fresh RPMI for 8 hours followed by infection with Chlamydia as previously described. Immediately following the infection the cells were put back in 2 mM thymididne in RPMI. After 12 hours, the cells were released with fresh media and samples were collected at the times indicated.

Fluorescence Ubiquinitation Cell Cycle Indicator

HeLa cells were transduced with Premo™ FUCCI Cell Cycle Sensor (Invitrogen) according to the manufacturer's instructions. When necessary, the cells were infected with *Chlamydia* after the transduction. The cells were then imaged live for 18 hours, collecting frames every 10 minutes. For infected cells, this time period captures 18-36 hours post infection. This experiment was repeated three times each for both uninfected and infected cell populations. Data sets were exported to an OMERO imaging data base (http://www.openmicroscopy.org/site/products/omero). Omero's quantification tools were used for the live cell intensity analysis.

Griseofulvin Treatment

HeLa cells were infected as previously described for 16 hours. The media was then changed to include 10 µM griseofulvin (Sigma) for the subsequent 20 hours. Cells were fixed in ice-cold methanol and stained.

Centrosome Calculations

Centrosome to nuclei distance was calculated by using ImageJ to draw a line from the closest centrosome to the nucleus. Centrosome spread was calculated by using 3D image stacks to produce a 2D binary image of the centrosomes. The 2D spread was calculated using the ImageJ plug-in “Hull and Circle.” A region of interest was drawn around the centrosomes and the area of the bounding circle was calculated from the minimal fitted polygon.

Statistical Analysis

Numerical data are presented as the mean ± SEM, and were analyzed by either the unpaired t-test or one-way ANOVA with a $p<0.05$ using GraphPad Prism4 software.

Table 2-1. Inhibitors used in experiments.

Inhibitor	Formula	Action
Cytochalasin D	$C_{30}H_{37}NO_6$	Disrupts actin filaments, preventing actin polymerization
Griseofulvin	$C_{17}H1_7ClO_6$	At low concentrations declusters centrosomes
Latrunculin A	$C_{22}H_{31}NO_5S$	Binds monomeric actin, preventing actin polymerization
Monastrol	$C_{14}H_{16}N_2O_3S$	Eg5 inhibitor that causes monopolar spindles during mitosis

Table 2-2. Peptide Inhibitors

Peptide	Sequence	MW	Charge	Purity
CPAF inhibitor	SEFYSPMVPHFWAELRNHYATSGLKS	3055.39	+2	>85%
Scrambled inhibitor	WNHSSTMGYFLLPAEVEKYSFSPHRA	3055.45	+2	>85%

CHAPTER 3
CHLAMYDIA INFECTION INDUCES HOST CYTOKINESIS FAILURE AT ABCISSION[1]

Introduction

Chlamydia trachomatis is a major human pathogen with biovars that can cause both sexually transmitted disease (STD) and trachoma, the leading cause of infectious blindness (Moulder, 1991; Hu et al., 2010) Infections caused by genital serovars of *C. trachomatis* can persist and lead to serious health sequelae such as pelvic inflammatory disease and tubal infertility in untreated women (Cates and Wasserheit, 1991). *Chlamydia* has also been clinically associated with cytologic cervical atypia (Kiviat et al., 1985) and epidemiologically linked to an increase in the risk for cervical cancer (Anttila et al., 2001; Smith et al., 2002; Madeleine et al., 2007). A direct molecular mechanism responsible for this link has yet to be described.

The obligate intracellular nature of the chlamydial infectious life cycle requires *Chlamydia* to reprogram many aspects of cellular function to render the cell hospitable to growth. *Chlamydiae* have multiple systems to secrete protein effectors into the host, modulating cellular behavior to create its unique intracellular niche. *Chlamydia* expresses both a type III secretion system as well as an uncharacterized type II dependent secretion system to efficiently deliver toxins/effectors to the cell to carry out these functions (Zhong, 2011; Dehoux:2011ep). These effectors induce a variety of cytopathic effects such as centrosome amplification, degradation of host proteins and multinucleation of the host cell (Greene and Zhong, 2003; Grieshaber et al., 2006; Paschen et al., 2008; Johnson et al., 2009). Multinucleated cells are common in all solid

[1] Previously published as: Brown, H.M., Knowlton, A.E., and Grieshaber, S.S. (2012). Chlamydial Infection Induces Host Cytokinesis Failure at Abscission. Cell Microbiol.

tumors and contribute to aneuploidy and chromosome instability (Weihua et al., 2011eg). The induction of multinucleation of the host cell during chlamydial infection is a potential contributing factor in the observed increased risk of cancer in infected patients.

Multinucleation can occur via cell fusion or cytokinesis failure, both of which have been shown to occur during viral infections. Disregulation of the cell cycle by viral infection leads to cytokinesis failure, and the membrane fusion events of budding viruses results in cell to cell fusion of neighboring cells (Duelli et al, 2007; Liu et al., 2005). Previous studies in *Chlamydia* suggest that either of these mechanisms could contribute to multinucleation. Egress of the chlamydial inclusion has been reported to be mediated, at least in part, by budding of the inclusion from the cell suggesting that *Chlamydia* may mediate membrane fusion events (KevinHybiske, 2007). Alternatively, we have recently determined that *Chlamydia* infection affects the cell cycle of the host cell by overriding the Spindle Assembly Checkpoint (SAC) causing infected cells to prematurely exit mitosis (Knowlton et al., 2011).

In this study we demonstrate that chlamydial induced multinucleation is entirely due to cytokinesis failure. Furthermore, we show that chlamydial induced multinucleation occurs due to failure late in cytokinesis at the abscission step. Finally, we establish that *Chlamydia* protease-like activity factor, CPAF, acts as an anaphase promoting complex by cleaving cyclin B1 and securin, allowing the chromosomes to prematurely separate. This activity drives cells through metaphase before the chromosomes are properly aligned and attached, leading to lagging chromosomes. The lagging chromosomes persist in the midbody between the newly formed daughter cells and ultimately interfere with abscission.

Results

Cytokinesis Fails Very Late in Infected Cells

We previously reported that chlamydial infected cells proceed through mitosis faster than uninfected cells (Knowlton et al., 2011). To determine if this impacts cell division, we directly examined infected dividing cells using live cell imaging. HeLa cells were transfected with GFP and infected with serovar L2. These cells were imaged every 10 minutes for 24 hours. Imaging was initiated at 20 hours post infection (hpi), as this is the start of the mature stage of the chlamydial infection. Images were collected for both infected and uninfected cells for a total of 41 infected cells and 39 uninfected cells that completed mitosis during imaging. The vast majority of the infected cells became multinucleated after mitosis (80.5% infected, Fig 3-1 C). This was a significant increase in multinucleation over the uninfected cell population (5.1% uninfected, Fig 3-1 C). In addition, cells were transfected with GFP-Bicaudal D1 and imaged 24 hpi every 15 minutes for 18 hours. Bicaudal D1 was used to localize the chlamydial inclusion (Matanis et al., 2002; Moorhead et al., 2007). We observed that multinucleation often occurred many hours after the completion of mitosis and in some cases occurred after differential expression of the GFP-Bicaudal D1 protein (Fig 3-1 A-B). The observed differential GFP-Bicaudal D1 expression between the apparent daughter cells that ultimately form a single multinucleated cell could be explained by two potential mechanisms; fusion of the closely associated cells after completion of cytokinesis or by failure late in the cytokinesis process after free diffusion is blocked by the formation of the midbody, a late cell division intermediate.

Multinucleation is Not Caused by Fusion

The genital biovars of *Chlamydia* are reported to egress from the cell without lysis, suggesting chlamydial infection may induce cell membrane fusion events in a manner similar to budding viruses (KevinHybiske, 2007; Todd and Caldwell, 1985). We employed a differential cell staining technique to determine if cell fusion occurs during infection. Two populations of cells were labeled with different fluorescent dyes and fusion events were scored by counting cells that fluoresced in both channels. HeLa cells were intrinsically labeled with either CytoTracker green or CytoTracker red fluorescent dyes. These two cell populations were then independently infected with *Chlamydia* L2. The two cell populations were trypsinized and co-plated onto coverslips 6 hpi and allowed to incubate for a total of 36 hours. These experiments were repeated with the genital serovar G but incubated for 48 hours, due to the slower growth rate. As a control to verify our ability to detect multinucleation, two uninfected cell populations were labeled with CytoTracker red or CytoTracker green, co-plated and subjected to an electrical current to induce fusion. Yellow stained cells indicating fusion between red and green dyed cells were enumerated at the indicated time points. No fusion could be detected in either serovars L2 or G infected samples with greater than 1000 multinucleated cells counted (Fig 3-1 D). Conversely, yellow stained cells indicating cell fusion were readily evident in the electro-fused samples. These data rule out fusion as a contributing mechanism for multinucleation.

Cytokinesis Fails After Ingression

Upon ruling out fusion as a mechanism for multinucleation, we sought to determine at which step cytokinesis fails in the chlamydial infected cells. Cytokinesis can be divided into multiple stages; specification of the cleavage plane and ingression of the cleavage furrow, followed by formation of the midbody and abscission (Normand and King,2010). Ingression of the cleavage furrow initiates with the formation of an actin-myosin ring during late anaphase in order to mechanically separate the daughter cells. To morphologically assess the structural organization of the contractile ring, infected cells were stained with fluorescently labeled phalloidin. The actin organization at the cleavage furrow appeared to be unperturbed by the chlamydial inclusion as there was no significant observable differences between infected and uninfected dividing cells (Fig 3-2A).

As an additional line of evidence that the actin cleavage furrow was not disrupted during infection, we compared infected cells to those treated with the actin depolymerizing compounds cyctochalasin D or latrunculin A. Disruption of the actin contractile ring during cytokinesis results in multinucleation and immediate arrest in G1 of the cell cycle (Lohez et al., 2003). Centrosome amplification induced by chlamydial infection is dependent on progression of the cell cycle into G2 (Johnson et al., 2009). We used this observation to assess the effects of cytokinesis failure induced by *Chlamydia* on cell cycle progression. As a measure of cell cycle progression we calculated the number of centrosomes per cell. The infected cells not treated with the actin depolymerizing drugs failed cytokinesis and had a clear increase in centrosome numbers (average centrosomes per cell 2.06, Fig 3-2B). However, infected cells treated with either cytochalasin D or latrunculin A became multinucleated but had no increase in

centrosome numbers over treated uninfected cells (average centrosome per cell 1.71, Fig. 3-2 B). The observation that the centrosome phenotype (no amplification) induced by disruption of the actin contractile ring was dominant over the chlamydial induced phenotype (amplification) demonstrates that chlamydial induced cytokinesis failure occurs at a step after formation and function of the contractile ring.

In addition to the lack of disruption of the actin cleavage furrow, the invaginated region of the cell did not appear to be sterically hindered by the chlamydial inclusion. To specifically address the effects of steric interference on cell division, we compared the multinucleation rate in cells infected with *Coxiella burnetii* with cells infected with *C. trachomatis* L2. *C. burnetii* is a bacterial pathogen with a eukaryotic intracellular life cycle that takes place in a vacuole termed the *Coxiella* containing vacuole (CCV) (Heinzen et al.,1999). Although the growth rate and characteristics of the intracellular niche differ between *C. trachomatis* and *Coxiella,* both organisms construct and maintain a large intracellular parasitophorous vacuole in which replication occurs (Heinzen et al.,1996). We measured the multinucleation rate of cells infected with C*. trachomatis* L2 and in agreement with previous reports, multinucleation is significant by 18 hpi (Fig 2D). The size of the inclusion at these early time points is similar to the size of the CCV at 96 hours due to *Coxiella's* slower growth rate. Cells infected with *Coxiella* for 96 hours displayed no increase in multinucleation compared to uninfected cells (Fig 3-2C and D). To specifically compare the steric effects of CCVs that were of similar size to the chlamydial inclusions, we measured the size of inclusions in chlamydial infected multinucleated cells at 18 hpi (average size of 5,588 μm2±450). We then calculated the multinucleation rate in *Coxiella* infected cells containing CCVs of comparable size

(average size of 6,429 μm^2±350, Fig 3-2C). There was no increase in multinucleation in this population of cells over uninfected cells. This demonstrates that simple steric effects exerted by the presence of the chlamydial inclusion does not account for the rate of cytokinesis failure observed.

The lack of cell cycle arrest, correct formation of the contractile ring, lack of steric interference from the chlamydial inclusion and the inhibition of diffusion prior to multinucleation all suggest that cytokinesis failure is occurring very late, likely at abscission.

Infected Dividing Cells Make Midbodies

Following formation of the actin-myosin contractile ring, cleavage furrow formation and ingression, the spindle microtubules are compacted to form an intracellular bridge containing densely packed microtubules termed the midbody (Caballe and Martin-Serrano, 2011). Abscission occurs after resolution of the membrane within the midbody to form the final independent daughter cells (Caballe and Martin-Serrano, 2011). To visualize the progression of cytokinesis, chlamydial infected cells were stained with anti-β-tubulin allowing us to quantify the effect of infection on the formation of the midbody, the last step before completion of cytokinesis. In uninfected HeLa cells, 74.2 ± 4.6% of post-metaphase mitotic cells possessed fully formed midbodies. This number increased to 92.2 ± 0.6% in the 36 hour chlamydial infected cell population (Fig 3-3A and B). UV treatment of uninfected cells was used as a control as UV treatment causes failure in cytokinesis by inducing DNA cross-bridging and forcing cells to abort cytokinesis at the abscission stage (Norden et al., 2006). We found that midbodies were present in 83.0 ± 1.2% of post-metaphase cells post UV exposure (Fig 3-3 B) indicating that cells that fail cytokinesis due to DNA bridges successfully form

midbodies. We also assessed midbody formation in cells that failed cytokinesis due to failure in the function of the actin contractile ring using cytochalasin D and latrunculin. These cells never progressed to midbody formation (Data not shown). The proper formation of midbodies during infection further indicates that chlamydial infected cells successfully proceeded through the actin-myosin contractile ring stage into this late stage of cytokinesis. The observation that chlamydial infection increased the number of cells with intact midbodies also suggested that there is a delay in the resolution of the midbody and that infected cells fail in cytokinesis at this stage. This is further supported by the observed differential expression of GFP observed in infected dividing cells because diffusion is limited by the compact midbody structure (Fig 3-1).

Lagging Chromosomes are Increased in Frequency in the Midbody of Infected Cells and Correlate with Multinucleation

Previous studies from our lab demonstrated that infected cells prematurely exit mitosis (Knowlton et al., 2011). A cell that exits mitosis before metaphase is complete can acquire chromosome segregation defects. These defects are commonly associated with cytokinesis failure as chromosome segregation errors can lead to chromosome non-disjunction and lagging chromosomes that bridge the midbody (King, 2008). We therefore examined dividing cells for the presence of DNA between the forming daughter cells. Cells infected with serovar L2 for 32 hours and uninfected cells were stained for DNA, microtubules and *Chlamydia* (Fig 3-4 A). Mitotic cells in these populations were quantified for the presence of DNA in the midbody between the two daughter cells. The infected cell population had a significant increase in the number of cells containing DNA in the midbody compared to uninfected (26.3% and 6.7% respectively, Fig 3-4B). Due to chromosome decondensation during mitotic exit limiting

detection, the number of cells with DNA in the midbody may be higher (Steigemann et al., 2009). In order to confirm that DNA in the midbody resulted in cytokinesis failure, we performed live cell imaging (Fig 3-4C). Uninfected cells succeed in mitosis 94.8% of the time, correlating with the low level of multinucleation observed in HeLa cells (Fig 3-4D). Surprisingly, we observed that uninfected cells displayed some level of DNA disorganization after metaphase. In this population 41.0% of successful cytokinesis events had evidence of DNA disorganization. The number of uninfected cells that failed cytokinesis was small (5.1%), however only half of these cells that failed cytokinesis had evidence of DNA disorganization suggesting that cytokinesis failure in uninfected cells was rarely caused by the presence of DNA in the midbody. In contrast, the rate of cytokinesis failure in the infected cell population rose to 80.5% with 93.9% of these demonstrating lagging DNA between daughter cells (Fig 3-4D). These data further suggest that the increase in lagging chromosomes and chromosome non-disjunction directly contributes to chlamydial induced cytokinesis failure.

Chlamydial Infected Cells do not Arrest in Metaphase

The spindle assembly checkpoint (SAC) regulates the timing of mitotic exit. This checkpoint blocks the progression at the metaphase to anaphase transition until chromosomes are properly aligned and have obtained bipolar attachment (McLean et al., 2011) This helps guarantee that the chromosomes are properly segregated to the poles and allows the chromosomes to be cleared from the cleavage furrow. As chlamydial infection increased the incidence of chromosomes found in the midbody between mitotic cells, we asked whether infection affects the SAC. To determine if *Chlamydia* infection is affecting the SAC, we triggered mitotic arrest with the drug monastrol. Monastrol specifically inhibits kinesin Eg5 resulting in the formation of

monopolar spindles (Kapoor and Mitchison, 2001). The disruption of bipolar spindle triggers the SAC, resulting in mitotic arrest in metaphase (Kapoor and Mitchison, 2001). Hela cells were infected with *C. trachomatis* serovar L2 and treated with monastrol for 24 hours. To assay for induction of the SAC, the mitotic index was measured by counting the percentage of cells in mitosis. Mitotic cells were stained with Hoechst to visualize DNA. The uninfected population had a mitotic index of 6.6 ± 0.3% which decreased to 4.4 ± 0.1% after infection (Fig 3-5A). Monastrol treatment led to an increase to 27.0 ± 1.1% and again when infected with *Chlamydia* this decreased to 21.9 ± 0.6%. These decreases showed statistical significance ($p<0.003$ and $p<0.01$, respectively). HeLa cells are a transformed cancer cell line and likely have changes in cell cycle check point control. Thus, we also looked at the effects of chlamydial infection on the SAC in a primary cell line. The mitotic index of primary human foreskin fibroblasts was 2.9 ±0.4% which dropped to 0.3 ± 0.1% when infected with *C. trachomatis* L2 (Fig 3-5B). Treatment of the fibroblasts with monastrol resulted in an increase of the mitotic index to 21.4 ± 0.8% indicating mitotic arrest. Monastrol treated infected primary fibroblasts showed a decrease in the mitotic index. The index dropped to 1.9 ± 0.1% suggesting that these cells no longer arrested in mitosis. Although fibroblasts are not a typical target cell of a natural chlamydial infection cell cycle control in all non-transformed cells is regulated by the same highly conserved checkpoint proteins. These data together demonstrate that infected cells do not arrest as efficiently during mitosis, even when the SAC is triggered.

We previously demonstrated that cyclin B1 and securin were degraded during chlamydial infection (Knowlton et al., 2011). Both of these proteins are important

regulatory components of the SAC, which controls mitotic exit. (Kim and Yu, 2011; Pines, 2011; van Leuken et al., 2008) The secreted chlamydial protease CPAF has been reported to degrade cyclin B1 (Balsara et al., 2006; Paschen et al., 2008). We reasoned that CPAF may be acting as an anaphase promoting complex mimic, causing premature exit from mitosis. The anaphase promoting complex/cyclosome (APC/C) is a ubiquitin ligase and regulates the SAC by targeting key molecules for degradation by the proteosome. (Baker et al., 2007; van Leuken et al., 2008) To test the hypothesis that CPAF is the chlamydial factor acting as an APC/C we purified a crude cytosolic fraction from chlamydial infected cells and tested the ability of this fraction to degrade cyclin B1 and securin. This fraction contains the active CPAF molecule that is secreted from *Chlamydia* (Huang et al., 2008). We analyzed the degradation of both cyclin B1 and securin by western blot analysis. Lysates from chlamydial infected cells but not uninfected cells resulted in degradation of both cyclin B1 and securin purified from mitotic uninfected cells (Fig 3-6A). We tested whether this degradation was due to CPAF proteolytic activity by using a specific CPAF inhibitory peptide. This peptide is derived from a self-inhibitory fragment of the CPAF zymogen that blocks access to the substrate binding pocket as described by Huang et al (Huang et al., 2008). This inhibitory peptide was demonstrated to have high potency against CPAF and is very specific as it does not affect the proteosome or CPAF from the closely related bacteria *C. caviae* (Jorgensen et al, 2011). Western blotting revealed that only infected lysates could actively degrade cyclin B1 and securin. This degradation could be inhibited by the CPAF inhibitory peptide, but a scrambled peptide did not block degradation. Furthermore, treatment of infected lysates with a protease inhibitor cocktail did not

inhibit degradation (Fig 3-6B), confirming that host proteases were not responsible for the degradation of cyclin B1 and securin. To test whether CPAF mediated degradation of cyclin B1 resulted in its loss of function we assayed for the activity of cyclin dependent kinase 1 (Cdk1). Cdk1 is active when bound to cyclin B1 and becomes phosphorylated on T161. We assessed the activity state of Cdk1 in infected mitotic cells using an antibody specific for this species. Western blotting revealed a drastic reduction in levels of phosphorylated active Cdk1 in chlamydial infected cells, supporting the hypothesis that degradation of cyclin B1 results in inactivation of the SAC (Fig 3-6C).

Cyclin B1-Cdk1 must accumulate and become active in order for the cell to enter mitosis (Gavet and Pines, 2010; Marangos and Carroll, 2008). To determine if degradation of cyclin B1 by CPAF alters the host cell's ability to enter mitosis we performed a mitotic index at various points after a thymidine release. Both uninfected and infected cells began to enter mitosis at 10 hour post release, but infected cells do not undergo a robust entry into mitosis (Fig 3-7A). Instead, infected cells show larger variability in the time it takes them to enter mitosis as is shown by the shallower slope on the graph (Fig 3-7A). Uninfected cells had a peek of mitotic entry at about 12 hours after release from the block. In comparison, the chlamydial infected cells still had not reached a peak of mitotic entry by 13 hours after block release. This delay tracks with cyclin B1 levels in these two populations. The uninfected cell population showed a larger and faster increase in cyclin B1 levels after the block then did the infected cells (Fig 3-7B). Additionally, we examined the length of S/G2 in uninfected and infected cells using the FUCCI cell cycle sensor (Sakaue-Sawano et al., 2008). HeLa cells were transduced with Premo FUCCI Cell Cycle Sensor and then infected with *Chlamydia*.

The length of S/G2 was calculated by measuring the time from the degradation of Cdt1-RFP (degraded at the beginning of S phase) to nuclear membrane breakdown. We determined that in uninfected cells S/G2 was 507.3 ±78.4 minutes, while infected cells had a longer S/G2 that lasted 774.6 ± 68.7 minutes (Fig 3-7C). Together these data demonstrate that the length of S/G2 is altered in infected cells and that this delay in entering mitosis correlates with a slower accumulation of cyclin B1.

Discussion

Multinucleation has been reported during chlamydial infections of cultured cells previously by Greene et al. and Sun et al. (Greene and Zhong, 2003; Sun et al., 2011). In this study we demonstrated that multinucleation during chlamydial infection is entirely caused by failure in cytokinesis and, in many cases, this failure occurs hours after apparent separation of the two daughter cells. By careful examination of the stages of cytokinesis in infected cells, we were able to determine that infected cells progressed through actin-myosin contractile ring formation and formed the typical condensed microtubule midbody structure that precedes the final stages of cell division, abscission. It is during this final stage that cytokinesis fails and multinucleation occurs. Abscission is irreversible for cytokinesis and is therefore regulated by a variety of pathways. By observing live infected cells by fluorescent microscopy we demonstrated that the population of cells failing cytokinesis were those that had DNA segregation errors caused by chlamydial infection. The presence of DNA in the midbody of dividing cells is a trigger to the cell to abort cytokinesis (Norden et al., 2006; Steigemann and Gerlich, 2009b). Our evidence supports the hypothesis that induction of DNA segregation errors during cytokinesis is a significant factor leading to cytokinesis failure in chlamydial infected cells. We demonstrated in previous studies that chlamydial infection shortens

mitosis of the host cell, causing a disorganized metaphase to anaphase transition (Knowlton et al., 2011). In this study we were able to connect the observed high rate of multinucleation to the induction of disorganized mitosis. During chlamydial infection both cyclin B1 and securin are degraded reducing the time dividing cells spend in metaphase (Knowlton et al., 2011). Here, we extended this observation demonstrating that the chlamydial toxin CPAF acts as an anaphase promoting factor mimic, directly degrading cyclin B1 and securin resulting in the inactivation of Cdk1. This activity is likely responsible for overriding the SAC allowing cells to proceed to anaphase with disorganized chromosomes, resulting in DNA segregation errors. A recent study from the Harrison lab suggested a role for steric effects of the chlamydial inclusion leading to asymmetric cleavage furrow formation (Sun et al., 2011). In our studies we focused on events midway through the infectious cycle, before the chlamydial inclusion became the majority of the cell volume. We directly compared the effects of *Coxiella* vacuoles of equal or greater size than those formed in chlamydial infected cells. In cells with large *Coxiella* vacuoles there was no increase in multinucleation, demonstrating that the presence of a large inclusion body is insufficient to cause multinucleation. It is possible that when the inclusion increases in size that steric effects also contribute to cytokinesis failure. Our results indicate that early exit from metaphase, caused by CPAF activity, is capable of causing lagging chromosomes that inhibit cytokinesis. However it is possible other chlamydial factors also contribute to cytokinesis failure. The Inc proteins CT223 and to a lesser extent CT224 and CT225 cause cytokinesis failure when ectopically expressed in mammalian cells (Alzhanov et al., 2009). The mechanism by which they

contribute to this failure is not known and ectopic expression is not always a reliable assay to assess the function of bacterial proteins.

Cyclin B1 and activated Cdk1 are required for cells to enter mitosis leading to the question of how degradation of cyclin B1 during the chlamydial infection affects entry into mitosis. In this study we show that infected cells have a delay in mitotic entry after S phase arrest and spend more time in S/G2 then uninfected cells. Cyclin B1 is synthesised in the cytosol but is shuttled into the nucleus. In the nucleus cyclin B1 and its partner active Cdk1 reach a threshold level triggering mitosis. We speculate that during chlamydial infection cyclin B1 levels are reduced as CPAF targets it for destruction in the cytosol, however, after cyclin B1 enters the nucleus it is protected from the activity of CPAF. This would explain the delay in mitotic entry. After NMBD cyclin B1 again becomes exposed to CPAF and is degraded pushing cells out of mitosis prematurely.

Overall, our data support a model where the combined cytopathic effects of chlamydial infection subsequently lead to multinucleation. In this model chlamydial infection leads to centrosome amplification and de-clustering of centrosomes (Grieshaber et al., 2006; Johnson et al., 2009; Knowlton et al., 2011). Additionally, CPAF degrades cyclin B1 and securin during mitosis leading to deactivation of Cdk1 and early exit from metaphase. Because of centrosome and spindle defects, the DNA is never properly aligned during metaphase leading to segregation errors during cytokinesis. These events ultimately lead to DNA bridging between daughter cells causing abscission failure (Fig 3-8). By inducing aneuploidy through lagging

chromosomes and cytokinesis failure, infection with *Chlamydia* may contribute to cellular transformation and cervical cancer.

The target of a naturally occurring chlamydial infection is the epithelial cell layer. These cells are highly differentiated and are reported to have a low population of replicating cells (Ramos et al., 2002). We speculate that the infection of replicating cells during a natural infection is a rare occurrence and therefore the induction of multinucleation is uncommon. However, HPV infection can drive cells out of quiescence and cause cells to reenter the cell cycle (Korzeniewski et al.,2011; McLaughlin-Drubin and Munger, 2009). We theorize that this population of cells would be more sensitive to cell cycle effects caused by chlamydial infection during a co-infection occurrence.

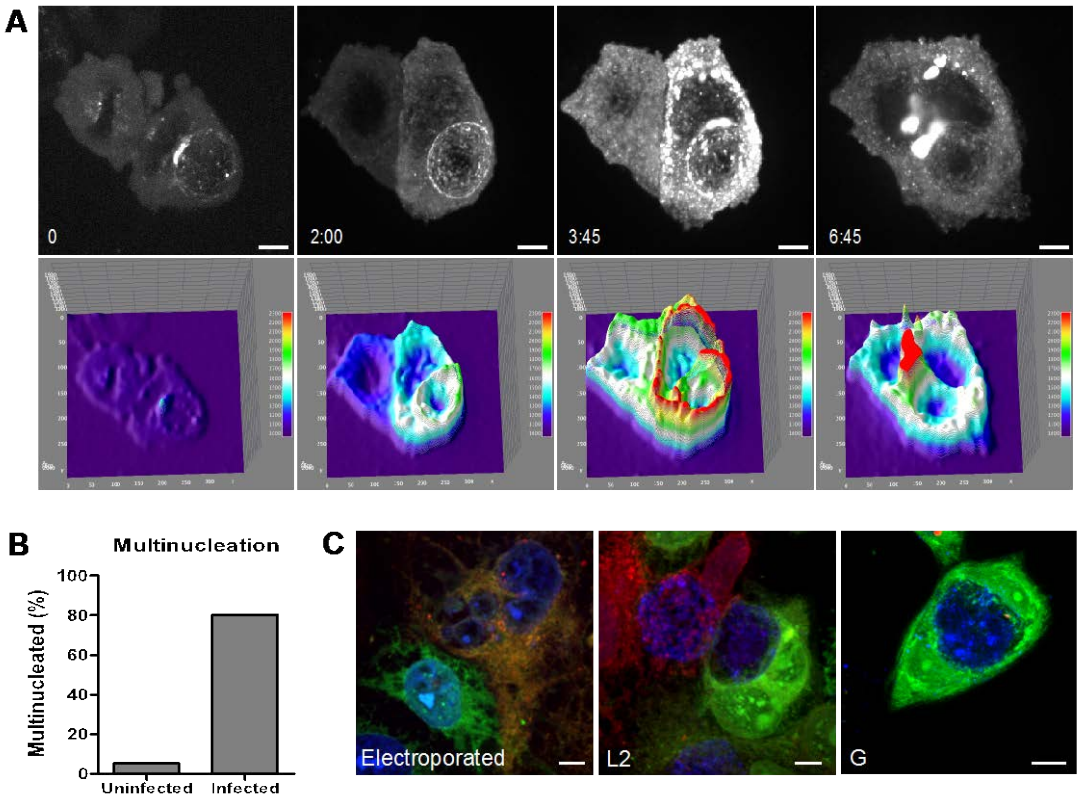

Figure 3-1. Multinucleation of host cells is due to cytokinesis failure and not cell fusion. A) HeLa cells were transfected with GFP-bicaudal D1 and then infected with *C. trachomatis* L2 for 24h. The cells were then imaged every 15 min for 18h. Images are time points from live cell imaging. Time 0 is started at telophase of the cell. Stars mark nuclei while the arrow points to the inclusion. GFP signal was graphed with an intensity plot to allow visual comparison of differing intensities between forming daughter cells. B) Live cell imaging was performed on *Chlamydia* infected HeLa cells. Beginning at 20 hpi cells were imaged every 10 minutes for 24 hours. Uninfected mitotic cells resulted in multinucleation in 5.1% of the cells, while infected mitotic cells became multinucleated 80.5%. n=39 and n=41, respectively. C) Two different populations of HeLa cells were stained with Cytotracker Red or Green. Cells were co-plated and either electroporated or infected with *C. trachomatis* L2 or G. Electroporation caused fusion as shown by the yellow multinucleated cell. Neither serovars of *C. trachomatis* induced fusion. 1000 multinucleated cells were counted and all multinucleated cells were due to cytokinesis failure.

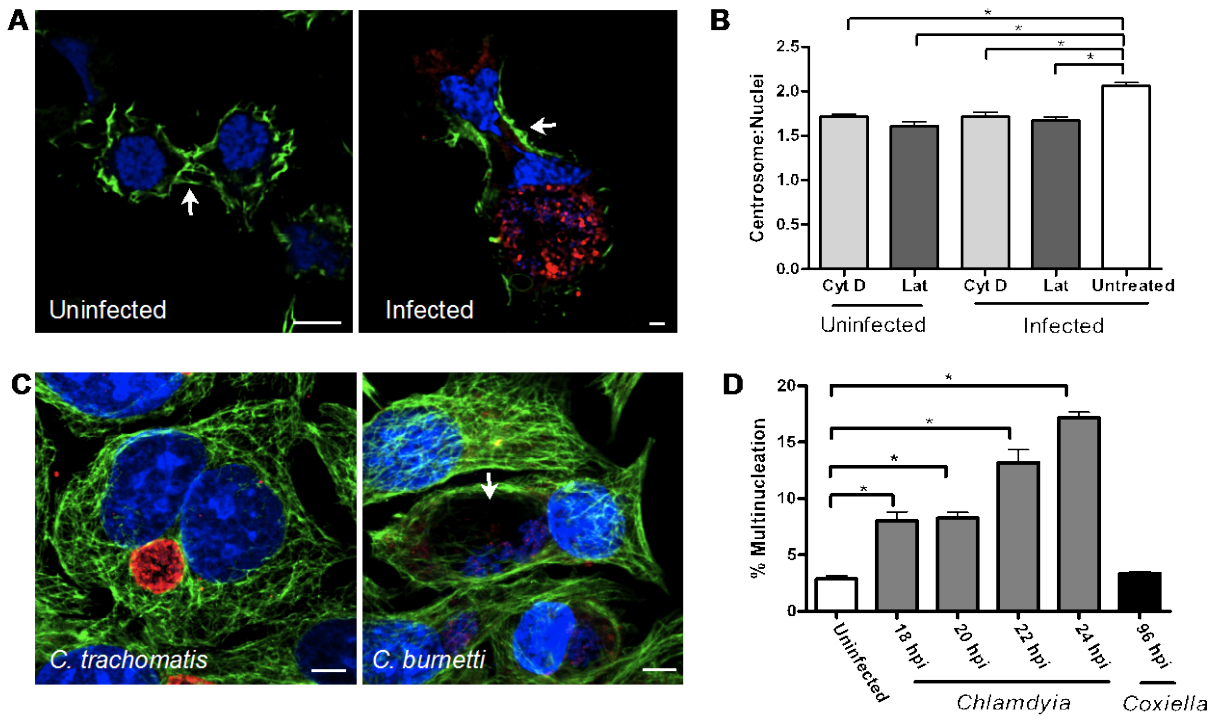

Figure 3-2. *Chlamydia* does not sterically hinder cytokinesis. A) HeLa cells were infected for 30 hours then fixed and imaged using immunofluorescence. Cells were stained with either phalloidin (green), Draq 5 for DNA (blue) and human serum for *Chlamydia* (red). The actin ring was able to properly form in *Chlamydia* infected cells. Arrows point to the actin ring. B) HeLa cells were treated with cytochalasin D or latrunculin A and the centrosome to nuclei ratio was evaluated using anti-ɣ-tubulin and Draq5. Uninfected cells and infected cells treated with cytochalasin D did not show a significant difference in centrosome to nuclei ratio, having a ratio of 1.7 ± 0.1 and 1.7 ± 0.1 respectively. Similarly, when cells were treated with latrunculin A, uninfected cells had a centrosome to nuclei ratio of 1.6 ± 0.1, while infected cells had a ratio of 1.7 ± 0.1 Untreated infected cells showed a significant increase with an average of 2.1 ± 0.1 centrosomes per cell p = 0.001. N= 3 experiments with at least 150 nuclei per experiment. C) Cells were infected with *Chlamydia* for 18 hours or *Coxiella* for 96 hours, then fixed. Cells were stained with anti-β-tubulin (green), human serum (red), and Draq5 (blue). The arrow indicates the location of the CCV. D) Cells were infected with *Chlamydia* or *Coxiella* for the indicated amounts of time and percent multinucleation of the population of infected cells were counted. Uninfected HeLa had a multinucleation rate of 2.9 ± 0.3% while infection increased multinucleation with time. The infected rates were 8.02 ± 0.81%, 8.26 ± 0.50%, 13.2 ± 1.3%, 17.2 ± 0.5% for 18, 20, 22, 24 hpi respectively. All chlamydial time points investigated demonstrated a significance of $p < 0.005$. *Coxiella* had a multinucleation rate of 3.4 ± 0.2%. N=3 experiments with at least 600 cells per experiment.

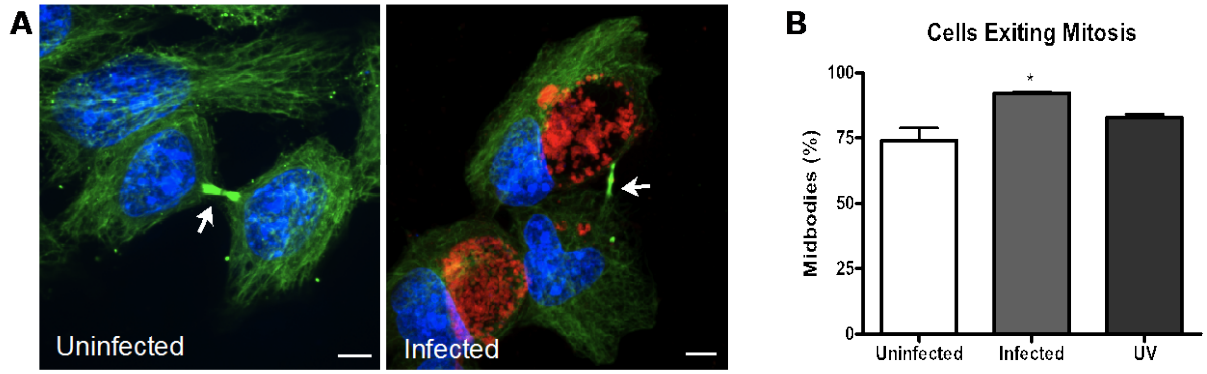

Figure 3-3. *Chlamydia* infected cells form midbodies. A-B) HeLa cells were infected for 30 hours then fixed and imaged using immunofluorescence. Cells were stained with anti-β-tubulin (green), human serum (red), and Draq 5 (blue). Arrows indicate location of the midbody. B) All cells that were post-metaphase in mitosis were evaluated for midbody formation. Midbodies were present in 74.2 ± 4.6 % of uninfected cells exiting mitosis, while this percentage rose to 92.2 ± 0.6% in cells infected with Chlamydia. A midbody was formed in 83.0 ± 1.2% of cells exiting mitosis that were exposed to UV light. Infected cells demonstrated a significant increase in midbody formation with a p=0.017. N= 3 experiments with at least 150 cells per experiment.

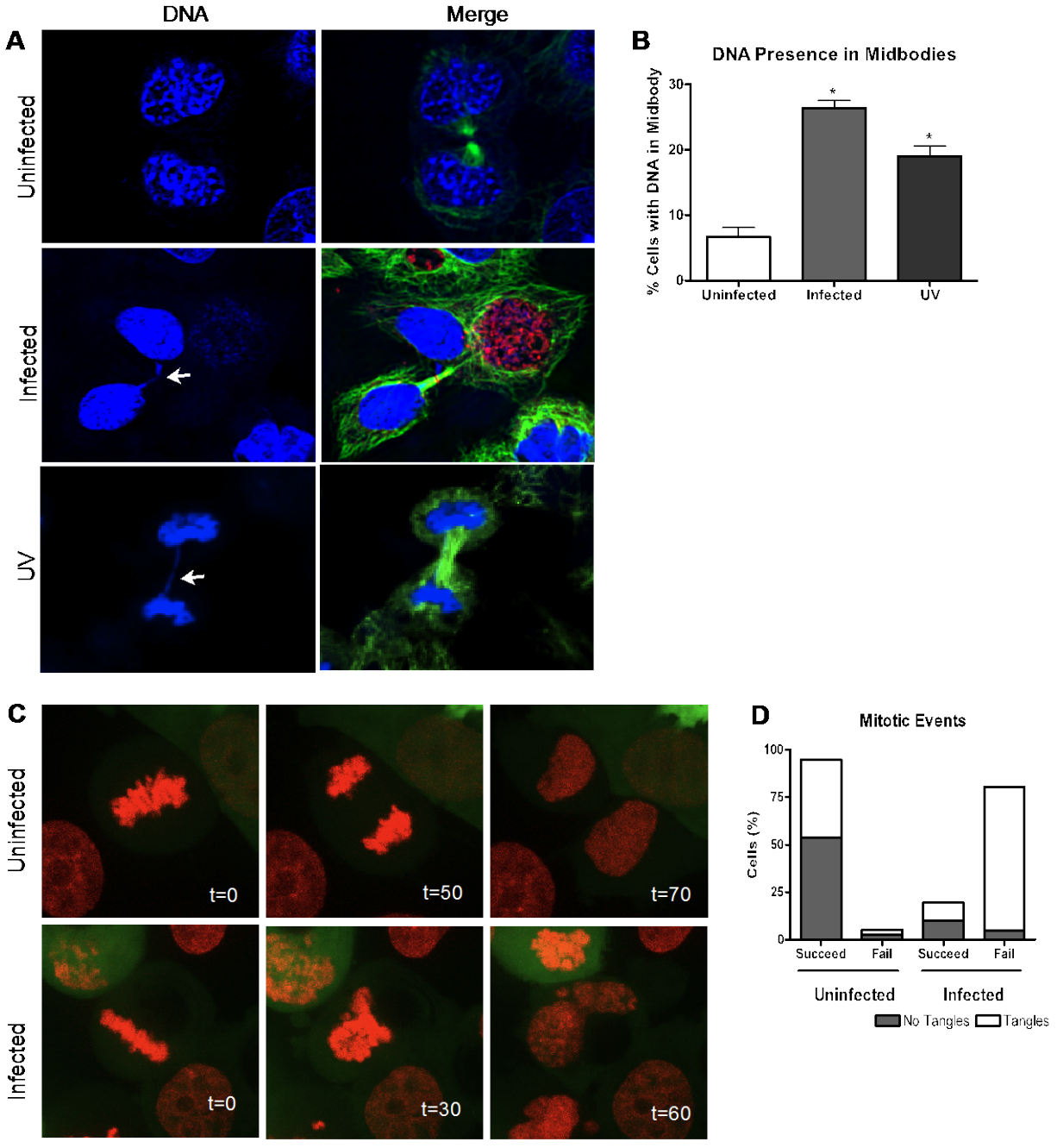

Figure 3-4. *Chlamydia* induces lagging chromosomes in infected cells. A) HeLa cells were infected for 30 hours then fixed and imaged. Conversely, uninfected cells were exposed to UV light for 3 minutes, allowed to grow for 24 hours and then fixed. Cells were stained with anti-β-tubulin (green), human serum (red), and Draq5 (blue) then examined in late telophase. Arrows indicate DNA bridging. B) Uninfected cells had DNA in the midbody 6.7 ± 1.5% of the time, while infected cells had DNA in the midbody 26.3 ± 1.2% of the time. When cells were exposed to UV light there was DNA present in the midbody 19.00±

1.5% of the time. N=3 experiments with at least 200 cells per experiment. A student t-test was performed with $p<0.02$. C) Stable RFP-H2B HeLa cells were transfected with GFP and infected with L2 for 20 hours. Cells were then imaged every 10 minutes for 24 hours. Panels show metaphase at time 0, followed by anaphase second and finally telophase of uninfected and infected cells. D) Cells were followed through mitosis with live cell imaging as shown in C. Cells were scored based on if they failed or succeeded in mitosis along with if DNA missegregation events were present. In uninfected cells, 94.9% of cells had successful mitosis, while only 19.5% of infected cells were successful. N=39 and N=41 cells, respectively.

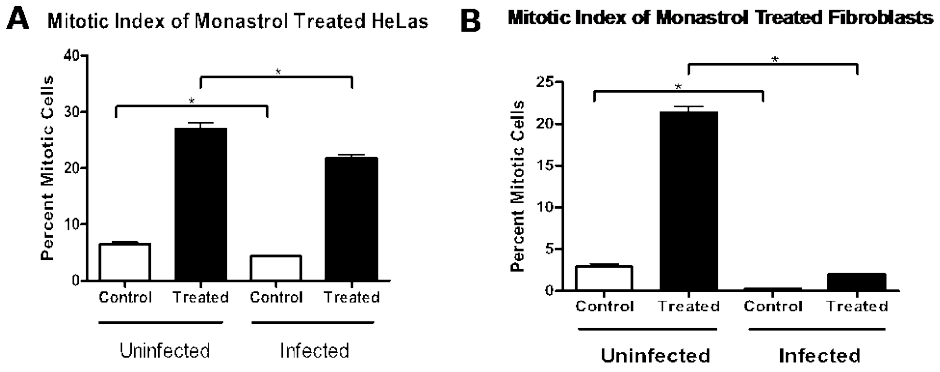

Figure 3-5. Chlamydia infection causes the premature exit of mitosis. HeLa cells were fixed 30 hpi and stained with anti-β-tubulin (green), human serum (red), and Draq5 (blue). Mitotic cells were compared to the total number of cells after infection and/or monastrol treatment. N= 3 experiments with at least 1500 cells per experiment. A) Uninfected HeLa cells had a mitotic index of 6.6 ± 0.3% which decreased to 4.4 ± 0.1% when infected, with a significance of $p=0.003$. When treated with monastrol 27.0 ± 1.1% of uninfected HeLa cells arrest in mitosis, but only 21.9 ± 0.6% of infected cells, $p<0.01$. B) Fibroblasts had a mitotic index of 2.9 ± 0.4% and 0.3 ± 0.1% for uninfected and infected cells, respectively, with a significance of $p<0.002$. Monastrol treated uninfected fibroblasts had a mitotic index of 21.4 ± 0.8%, while infected fibroblasts had a mitotic index of 1.9 ± 0.03%, with $p<0.0001$.

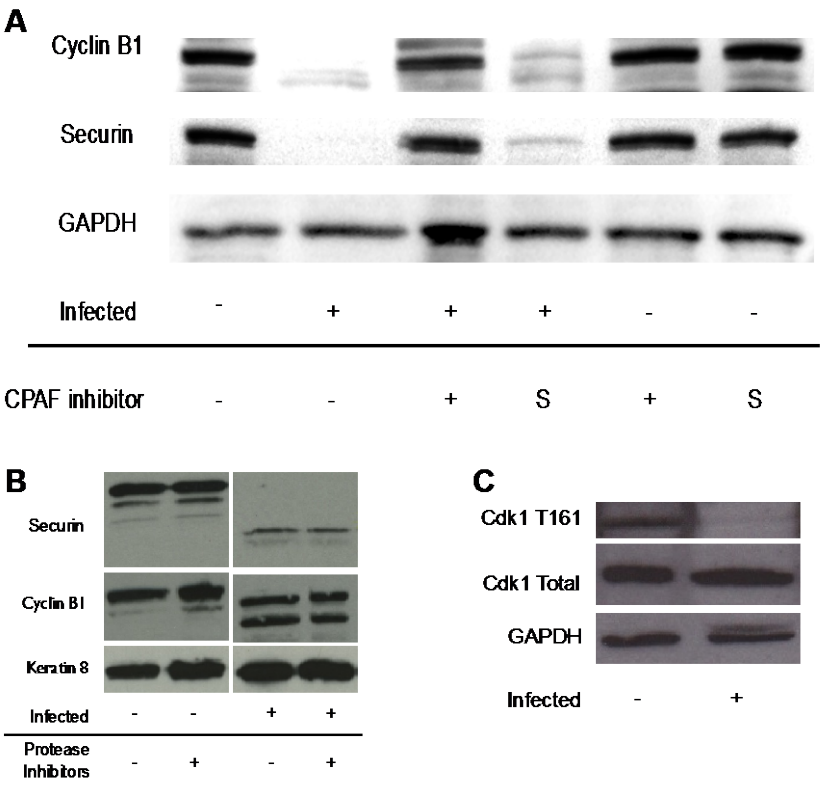

Figure 3-6. CPAF degrades cyclin B1 and securin. A) A cell-free degradation was performed and analyzed by western blot. Cyclin B1 and securin were degraded by infected cell lysate. Degradation could be blocked with a small peptide inhibitor of CPAF. B) Same experiment as A, but infected cell lysate was treated with a protease inhibitor cocktail. C) Mitotic shake-offs were performed to harvest proteins from uninfected and infected cells. Western blots show that the level of Cdk1 is unchanged due to infection, but the active T161 form of Cdk1 is not present in infected cells.

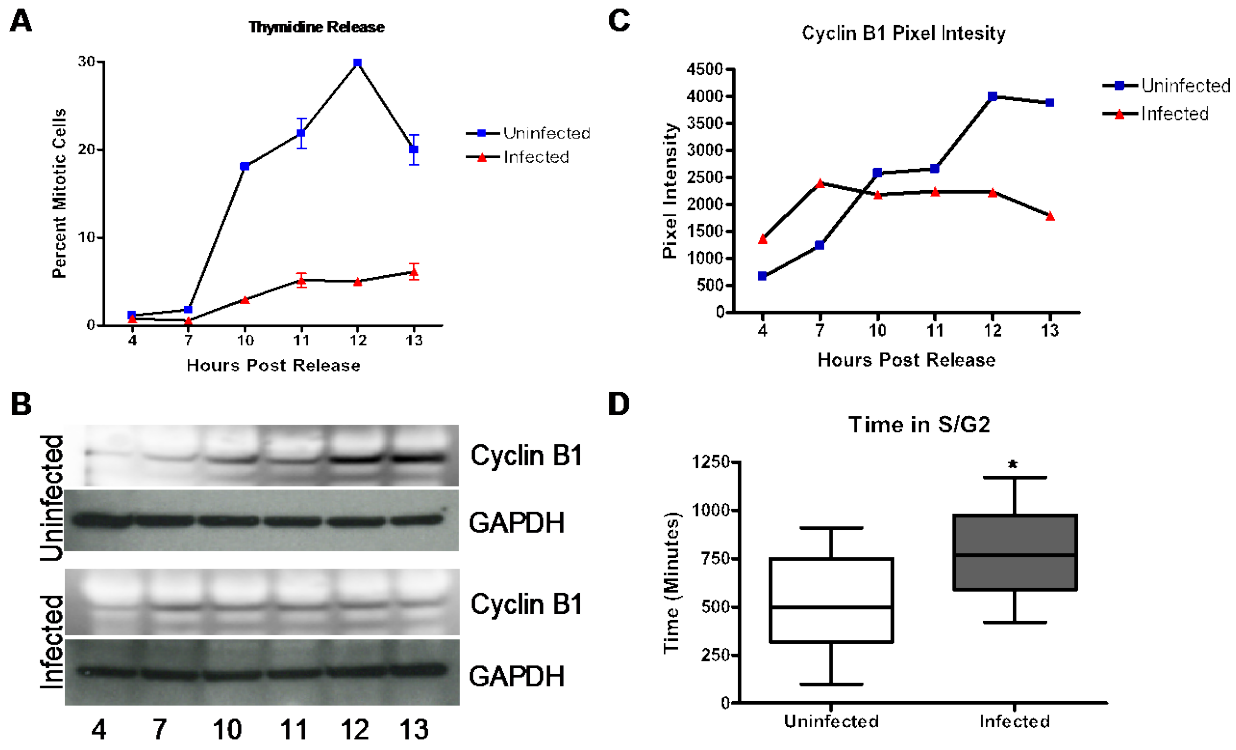

Figure 3-7. Host cell entry into mitosis. A-B) A double thymidine block and infection was performed on HeLa cells. Cells were released and samples were collected at time points indicated. A) Cells were fixed and stained for anti-β-tubulin (green), human serum (red), and Draq5 (blue) and a mitotic index was performed. In uninfected cells, a significant increase in mitotic cells begins at 10 hours post release, with the peak of mitosis occuring 12 hours after release from thymidine. Infected cells begin entering mitosis at 10 hours as well, but are not tightly synchronized. B-C) Western blot analysis was performed on uninfected and infected cell lysates. Cyclin B1 levels were evaluated for cells entering mitosis. D) HeLa cells were transduced using the FUCCI system and infected with *Chlamydia*. Starting 18 hpi, the cells were imaged every 10 minutes for 18 hours. The duration of S/G2 was calculated from the time of Cdt1-RFP degredation to mitotic entry (nuclear membrane breakdown). Uninfected cells were in S/G2 for 507 ± 78.4 minutes while infected required 774.6 ± 68.7 minutes with N=11, 13 respectively. The duration was significantly different with $p<0.02$.

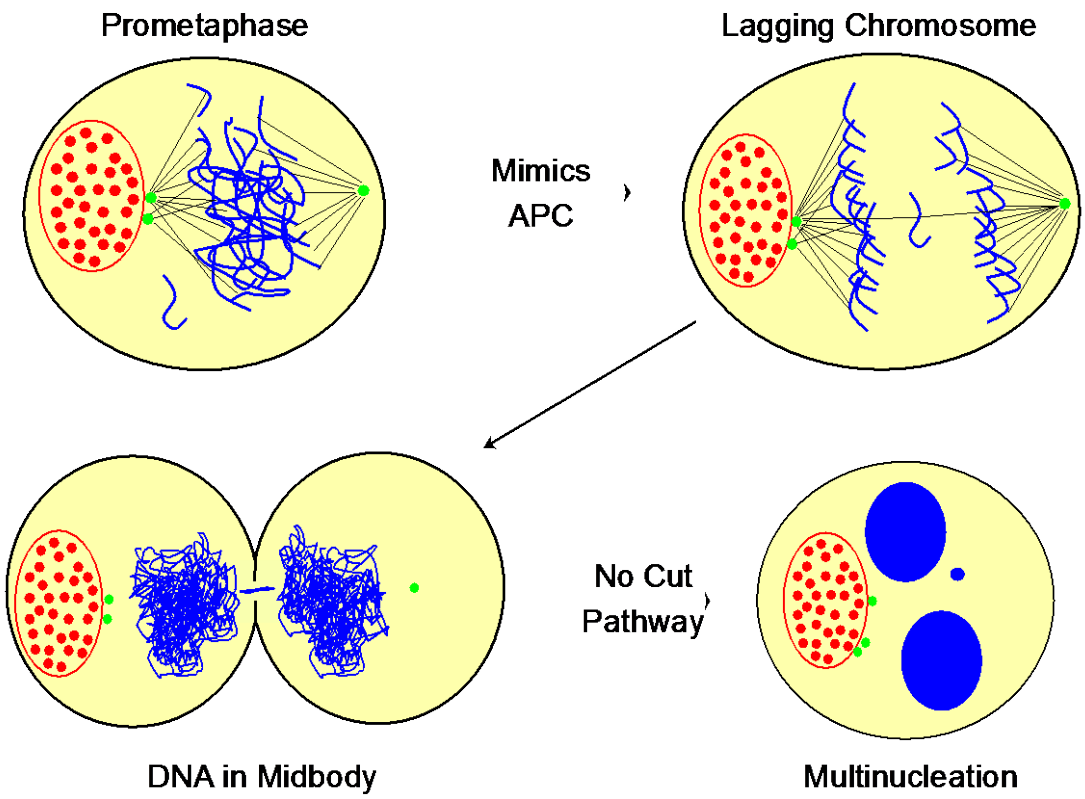

Figure 3-8. Model of chlamydial induced multinucleation**.** Chlamydial inclusions (red) secrete CPAF into the cytoplasm of the host cell (yellow). CPAF mimics the APC causing the cell to exit metaphase before microtubules (black) attach to the kinetochores of the chromosomes (blue). Furthermore, premature exit from metaphase does not allow supernumerary centrosomes (green) to cluster. This results in lagging chromosomes that become trapped in the midbody of the host cell. The host cell aborts abscission via the No Cut Pathway in order to protect the DNA. Lagging chromosomes can result in micronuclei.

CHAPTER 4
DECLUSTERING OF HOST CELL CENTROSOMES IS NOT CONSERVED AMONG SPECIES OF CHLAMYDIA

Introduction

Chlamydia trachomatis is an obligate intracellular pathogen that is the causative agent of the sexually transmitted infection (STI) Chlamydia (Moulder, 1991). Chlamydia is the most common bacterial STI with an estimated 4 million cases annually in the United States (Belland et al., 2004). Furthermore, *C. trachomatis* is of significant clinical importance because infection can result in pelvic inflammatory disease, ectopic pregnancy, and infertility (Cates and Wasserheit, 1991). More recently, *C. trachomatis* has been epidemiologically linked to cervical and ovarian cancer (Koskela et al., 2000; Anttila et al., 2001; Alibek et al., 2012).

Chlamydial infection overrides the Spindle Assembly Checkpoint (SAC), amplifies centrosomes and prevents clustering of the centrosomes (Grieshaber et al., 2006; Johnson et al., 2009; Knowlton et al., 2011; Brown et al., 2012). Additionally, we demonstrated that these phenotypes may act together to cause multinucleation of infected cells (Brown et al., 2012). Multinucleated cells are common in all solid tumors and contribute to aneuploidy and chromosome instability (Weihua et al., 2011).

The chlamydial factors involved in the induction of these phenotypes leading to multinucleation and aneuploidy are currently unknown. Therefore, we investigated the ubiquity of the induction of these phenotypes across divergent chlamydial species. We compared the ability of *C. trachomatis* L2, *C. muridarum* (MoPn) and *C. caviae* (GPIC) in their ability to induce centrosome amplification. *C. muridarum* is a mouse-specific pathogen that is evolutionarily closely related to *C. trachomatis.* Its genome has been sequenced, and 98.7% of the genes are conserved between *C. trachomatis* and *C.*

muridarum (Read et al., 2003). *C. muridarum* is well studied and used as the mouse model for human genital tract infection. GPIC was chosen because it is more distantly related to *C. trachomatis,* with 91.1% of genes conserved between the species (Read et al., 2003). GPIC is closely related to *C. pneumoniae,* a human pathogen of the respiratory tract. Guinea pig infection with GPIC is the best animal model for human *C. pneumoniae* infection. All three species are well studied and grow at a similar rate, requiring approximately 48 hours to complete infection. Therefore, these species are easy to compare at the same developmental stage.

Although the genus *Chlamydia* has a large host diversity, wide tissue tropism and varied disease pathology, there is a high conservation of genes among the different species. GPIC, MoPn and *C. trachomatis* have 810 genes conserved between all three (Read et al., 2003). Despite having highly conserved genes, there is variation in expression of genes between species. For example, despite the fact that GPIC contains an identical set of glycogen-metabolizing genes, GPIC does not accumulate glycogen like *C. trachomatis* and *C. muridarum* (Moulder, 1991; Iliffe-Lee and McClarty, 2000). Another variation among *Chlamydia spp.* is in their Inc proteins (Inclusion membrane proteins), which are a vital part of chlamydial-host interactions due to their localization to the inclusion. *C. trachomatis* has 20 confirmed Inc proteins, but only a small subset is conserved among other species (Dehoux et al., 2011). Finally, the appearance of the inclusion varies between species. Phenotypically, the L2 and MoPn inclusions form a smooth sphere, while GPIC forms a multi-lobed, raspberry-like structure.

In this study we demonstrate that changes in the host cell due to *Chlamydia* infection is not conserved among species. We found that all three species caused the same rate of centrosome amplification and prematurely exit mitosis, but *C. trachomatis* had the highest rate of centrosome declustering that correlated with rates of multinucleation.

Results

Chlamydia Species Cause Different Rates of Multinucleation

C. trachomatis causes multinucleation through cytokinesis failure in a majority of the cells that undergo mitosis (Greene and Zhong, 2003; Brown et al., 2012). In order to determine if this phenotype was conserved throughout the *Chlamydia* genus, we determined the multinucleation rate of the closely related species *C. muridarum* (MoPn) and the more divergent *C. caviae* (GPIC). Uninfected cells have a multinucleation rate of 2.9 ± 1.0%. We determined that at 40 hours post infection (hpi) GPIC and MoPn cause multinucleation rates of 10.9 ± 0.9 % and 28.1 ± 0.6%, respectively. These multinucleation rates are significantly lower than the 64.7 ± 2.5% that is observed in L2-infected cells (Figure 4-1B). All three species have similar growth rates, but to ensure our findings were not due to differences in inclusion size we measured the area of the inclusions. The inclusion sizes for GPIC, MoPn and L2 were 328 ± 93 μm^2, 360 ± 122 μm^2, and 351 ± 139 μm^2 respectively. The inclusion sizes were not significantly different with a p-value of >0.3. We aimed to determine the differences in host-pathogen interactions between species from these findings.

Our previous studies suggested that multinucleation results from a combination of changes to the cells that cause missegregation of the chromosomes during mitosis. Therefore, we examined if other chlamydial infection phenotypes varied between

species. We performed a mitotic index to determine if the species of *Chlamydia* caused mitosis to occur at different rates. We found that all three species of *Chlamydia* tested caused a comparable rate of mitosis with no significant difference when comparing the mitotic index (Figure 4-1C). Similarly, centrosome amplification did not vary between *Chlamydia* species (Figure 4-1D). Finally, we observed abnormal spindles, or cells with greater that two spindle poles, to investigate declustered centrosomes. We found a dramatic difference in the species' ability to decluster supernumerary centrosomes. While L2 cause greater than two spindle poles in 70.1 ± 2.6% of mitotic cells, GPIC and MoPn only caused greater than two spindle poles in 31.8 ± 1.8% and 51.0 ± 2.0% of mitotic cells, respectively (Figure 4-1E). We hypothesize that the difference in centrosome declustering accounts for the varied multinucleation because the rate of abnormal spindles mimicked the rate of multinucleation.

Treating Cells with Griseofulvin Increases Multinucleation Rate

We hypothesized that if we induced centrosome declustering in GPIC-infected cells, we would observe the same rate of multinucleation as compared to L2-infected cells. Therefore, we treated infected cells with 20 μM griseofulvin to decluster centrosomes. GPIC induced multinucleation increased from 10.9 ± 0.9 % when untreated to 42.6 ± 1.4% when treated with griseofulvin. This multinucleation rate was not a significant difference compared to 49.2 ± 6.4% for L2-infected and griseofulvin treated cells (Figure 4-2B).

Next, we compared abnormal spindles in infected and griseofulvin-treated cells to ensure that this change in multinucleation was indeed due to declustering of centrosomes. Uninfected cells treated with griseofulvin had greater than two spindles poles in 52 ± 3% of mitotic cells. When cells were infected with GPIC and treated with

griseofulvin this rate increased to 77 ± 10%. Cells infected with L2 and treated with griseofulvin had a multipolarity rate of 77 ± 5% which was not significant compared to the GPIC group (Figure 4-2C).

The mitotic index was calculated from these same cells to ensure that a change in mitotic index for the two species had not occurred. The mitotic index for uninfected, griseofulvin-treated cells was 26.2 ±0.6% that decreased to 16.8 ± 1.4% for GPIC-infected cells and 19.5 ± 5.3% for L2-infected cells (Figure 4-2D). There was no significant difference between the species, and the lowered mitotic index indicates that both species of *Chlamydia* can override the SAC. The SAC should be activated in griseofulvin-treated cells due to declustered centrosomes. We conclude that the varying rates of multinucleation are due to the species' ability to decluster centrosomes.

Centrosomes Are Mislocalized and Declustered during Interphase

Centrosomes are normally located in a perinuclear position during interphase. We hypothesized that abnormal spindles would correlate to mispositioned centrosomes in the cell during interphase. We measured the centrosome to nucleus distance in HeLa cells infected with the different species of *Chlamydia* to test this hypothesis. As expected, 79% of the centrosomes in uninfected cells were within 1 μm of the nucleus. When infected with GPIC or MoPn the centrosomes were pulled away from the nucleus, but 75% and 81% of GPIC- and MoPn-infected cells positioned centrosomes within 5 μm of the nucleus. Conversely, when the cells were infected with L2, only 55% of the centrosomes were within 5 μm of the nucleus. Furthermore, there was a long drawn out tail to the histogram with centrosomes up to 19 μm away from the nucleus [Figure 4-3B]. The centrosome to nucleus distance between species was

significantly different by ANOVA. This suggests that the inclusions formed by the chlamydial species interact differently with the centrosome.

Previously we demonstrated that *C. trachomatis* L2 infection causes a declustering of centrosomes during interphase in neuroblastoma cells (Knowlton et al., 2011). Neuroblastoma cells have around 8-10 centrosomes and are therefore a useful cell line to study declustered centrosomes. The extent of centrosome declustering is determined by measuring the space occupied within a bounding circle. Uninfected cells clustered the centrosomes within 148 ± 84 μm^2 (Figure 4-4B). There was not a significant difference compared to uninfected cells in centrosome spread when cells were infected with GPIC or MoPn. The GPIC centrosome spread was 141 ± 90 μm and MoPn was 122 ± 71 μm. When neuroblastoma cells were infected with L2 the centrosome spread increased to 229 ±189 μm. There was a long tail of extremely spread out centrosomes, similar to what was observed in the centrosome to nuclei distance. The centrosome spread increase was significant with a p-value of <0.002.

Declustered Centrosomes Cause a Disorganized Mitosis

All species of *Chlamydia* drive cell progression through mitosis more rapidly than uninfected cells, but vary in their ability to decluster centrosomes. Therefore, cells infected with L2 should undergo a more disorganized mitosis compared to the other species of *Chlamydia*. We categorized the mitotic cells in each population to determine if the species of *Chlamydia* altered the phases of mitosis differently. In uninfected cells, 11.0 ± 3.2% were in prophase, 22.8 ± 1.3% in prometaphase, 36.3 ± 5.0% in metaphase, 14.6 ± 1.2% in anaphase, and 15.3 ± 4.1% in telophase. The phases of mitosis did not change when cells were infected with GPIC. In GPIC-infected cells, 5.6 ± 2.3% were in prophase, 28.7 ± 1.9% in prometaphase, 38.8 ± 2.8% in metaphase,

16.7 ± 3.1% in anaphase, and 10.1 ± 1.1% in telophase. However, when cells were infected with MoPn or L2, there was a change in the phases of mitosis, with a significant shift from metaphase to prometaphase. In MoPn-infected cells 8.2 ± 0.1% were in prophase, 43.6 ± 2.5% in prometaphase, 28.4 ± 3.3% in metaphase, 9.6 ± 1.0 % in anaphase, and 10.1 ± 2.2% in telophase. Similarly, in L2-infected cells 5.1 ± 1.0% were in prophase, 51.9 ± 1.4% in prometaphase, 26.2 ± 1.9% in metaphase, 8.1 ± 1.2 % in anaphase, and 8.7 ± 1.4% in telophase (Figure 4-5A).

Due to the dramatic change in the prometaphase to metaphase ratio, we examined only those two phases. Uninfected cells have a prometaphase to metaphase ratio of 0.6 ± 0.1 (Figure 4-5B). GPIC did not exhibit a significant difference with a ratio of 0.7. However there was a dramatic difference in MoPn- and L2-infected cells compared to uninfected cells with a ratio of 1.5 ± 0.3 and 2.0 ± 0.1 with p-values of <0.05 and <0.001, respectively. The difference between prometaphase and metaphase is that in metaphase, chromosomes are aligned at the metaphase plate. This shift suggests that MoPn- and L2-infected cells require more time to organize their chromosomes, but because of the shortened mitosis, some cells go directly from prometaphase to anaphase.

If cells exit mitosis before chromosomes are aligned, then we should observe more DNA segregation errors. To test this hypothesis, we scored cells exiting mitosis for DNA bridges. In uninfected cells DNA bridges were present in 6.4 ± 1.1% of cells that exited mitosis (Figure 4-6B). This increased to 13.5 ± 1.6% in GPIC-infected cells, 24.8 ± 2.5% in MoPn-infected cells and 29.7 ± 3.8% in L2-infected cells. MoPn and L2 infected populations demonstrated a significant increase with a p-value >0.005. These

numbers suggest that centrosome declustering is necessary for DNA bridges in infected cells.

Discussion

We have previously shown that *C. trachomatis* L2 causes multinucleation through DNA bridging causing cytokinesis failure (Brown et al., 2012). In this study we demonstrated multinucleation of the host cell and declustered centrosomes are not conserved among *Chlamydia spp*., but all species override the SAC and amplify centrosomes. To determine if declustered centrosomes correlated to increased multinucleation rate, we infected cells with GPIC and treated the cells with the centrosome-declustering agent griseofulvin. Host cells infected with GPIC and treated with griseofulvin demonstrated a similar rate of multipolar mitosis and multinucleation as *C. trachomatis* infected cells. These findings suggest that declustered centrosomes are required for the high rates of multinucleation in host cells.

Normally, cells with amplified centrosomes have the innate ability to cluster supernumerary centrosomes to suppress multipolar spindles (Ring et al., 1982). Since *C. trachomatis* amplified centrosomes but did not cluster centrosomes, infection must disrupt the clustering process (Quintyne et al., 2005; Saunders, 2005). The host cell demonstrates defects in centrosome clustering beginning in interphase, long before the mitotic spindle has formed. In our studies, we observed that centrosomes were pulled away from the nucleus and spread apart due to *C. trachomatis* infection. Declustered centrosomes would require correction before mitosis for a normal cell division.

The cells' ability to maintain clustered supernumerary centrosomes is an active process that requires both an intact SAC and proper organization of the spindles by microtubule motor proteins (Kwon et al., 2008). *C. trachomatis* infection overrides the

SAC but does not affect nuclear mitotic apparatus protein (NuMa) or dynein trafficking (Knowlton et al., 2011; Brown et al., 2012). In this study we demonstrated that all three chlamydial species studied caused a decreased mitotic index, indicating a shortened mitosis and overriding the SAC. We hypothesize that in *Chlamydia* infected cells, the inclusion's interaction with the centrosomes may cause the variation observed in declustering.

Declustered centrosomes promote a disorganized mitosis. Therefore we hypothesized that declustered centrosomes would correlate to a shift from metaphase to prometaphase in infected cells. In this study we demonstrated that *C. trachomatis* had the largest metaphase to prometaphase shift that correlated to declustered centrosomes. Finally, we investigated variation in DNA tangles due to infection with different species. *C. trachomatis* causes DNA in the midbody of mitotic host cells that results in cytokinesis failure (Brown et al., 2012). In this study we observed that DNA in the midbody is correlated to declustered centrosomes. *C. caviae* infected cells decluster centrosomes less than *C. trachomatis* infected cells, which results in a lower rate of multinucleation. Declustered centrosomes promote multipolar and pseudo-bipolar mitosis, resulting in chromosomal segregation errors. The presence of chromosomal segregation errors cause the cell to fail in cytokinesis in order protect the integrity of the DNA through the NoCut pathway (Norden et al., 2006; Steigemann and Gerlich, 2009a).

We therefore propose a new model in which all species of *Chlamydia* override the SAC and amplify centrosomes, but the studied species cause varied degrees of declustered centrosomes that correlate to the rate of multinucleation (Figure 4-7).

Therefore during a *C. trachomatis* infection, host cells enter mitosis with declustered centrosomes. Before the cell has time to correct the declustered centrosomes, *Chlamydia* bypasses the SAC. This results in lagging chromosomes and cytokinesis failure. Conversely, GPIC and MoPn decluster centrosomes less, so when the SAC is bypassed there are fewer lagging chromosomes and cytokinesis is completed.

Previous *C. trachomatis* infections have been epidemiologically linked to cervical cancer. In this study we have elucidated a mechanism by which *Chlamydia* could contribute to cellular transformation. Infection with *C. trachomatis* may contribute to cellular transformation and cervical cancer, by inducing aneuploidy through DNA segregation errors and cytokinesis failure

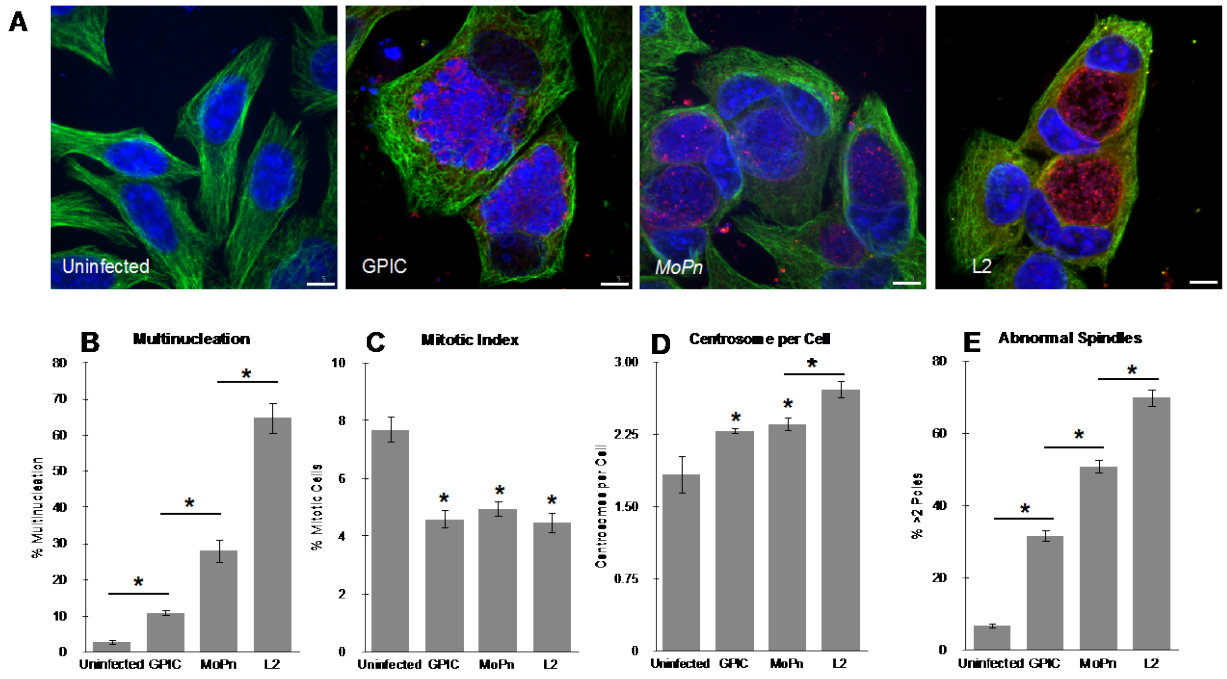

Figure 4-1. Multinucleation with different species A) HeLa cells were infected with *Chlamydia trachomatis* (L2), *C. muridarum* (MoPn) or *C. caviae* (GPIC) for 40 hours. Cells were stained with anti-β-tubulin (green), human serum (red), and Draq5 (blue). B) Uninfected cells had a multinucleation rate of 2.9 ± 0.6%, which increased to 64.7 ± 2.5% in L2 infected cells. GPIC and MoPn also demonstrated an increase multinucleation rate of 10.9 ± 0.9 % and 28.1 ± 0.6%. Compared to uninfected, GPIC, MoPn, and L2 infected cells were significantly different (ANOVA). N=3 experiments with at least 600 cells per experiment. C) Number of mitotic cells compared to total cells was counted for the mitotic index. Uninfected cells had a mitotic index of 7.7 ± 0.5%, while GPIC, MoPn and L2 had a mitotic index of 4.6 ± 0.2%, 5.0 ± 0.3% and 4.5 ± 0.4%, respectively. There was significance difference in means between uninfected, GPIC, MoPn, and L2 (ANOVA), but there was not a significant difference between the species. N=3 experiments with at least 1500 cells per experiment. D) Percent of mitotic cells that contained more than 2 spindle poles were evaluated. Uninfected cells had multipolar spindles 6.8 ± 0.9% of the time. When infected with the different species the abnormal spindle rate was 31.8 ± 1.8% (GPIC), 51.0 ± 2.0% (MoPn) and 70.1 ± 2.6% (L2). There was significance difference of means between uninfected, and all species of Chlamydia (ANOVA), and a significance of $p<0.001$ between species. N=3 experiments with at least 100 cells per experiment. E) Centrosomes per cell were counted to determine the centrosome amplification in infected cells.

Uninfected had 1.8 ± 0.2 centrosomes per cell. The infected cells had 2.3 (GPIC), 2.4 ± 0.1 (MoPn) and 2.7 ± 0.1 (L2) centrosomes per cell. There was significance difference in means of uninfected and all species (ANOVA), a significance of $p<0.005$ of L2 compared to GPIC or MoPn. There was not a significant difference between GPIC and MoPn. N=3 experiments with at least 150 cells per experiment.

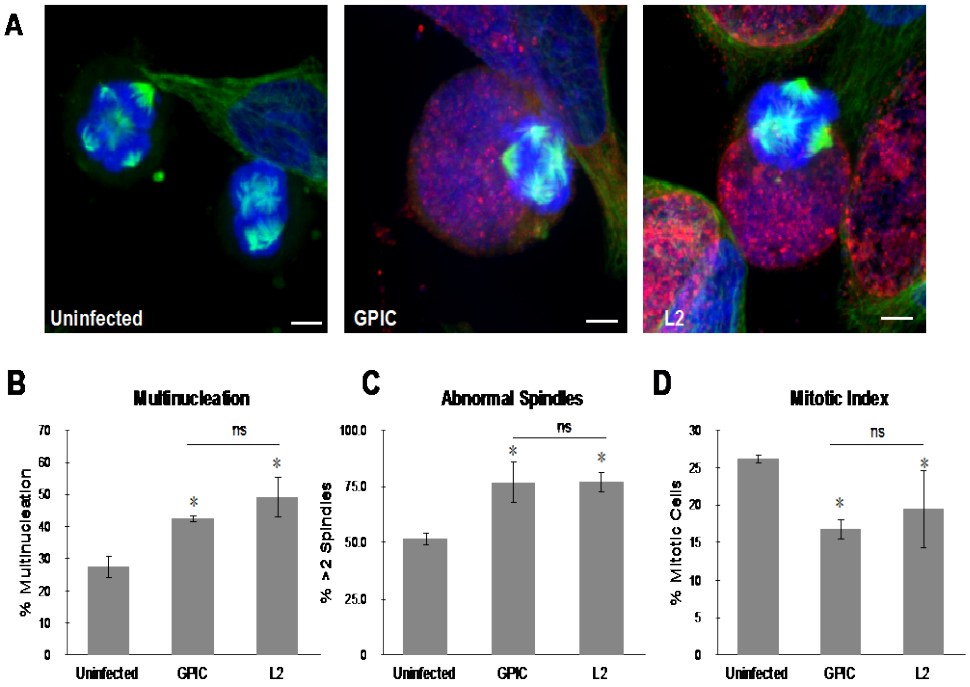

Figure 4-2. Declustering of centrosomes by griseofulvin. A) HeLa cells were infected with L2 or GPIC for 24 hours and then treated with 20 μM griseofulvin for a further 16 hours. Cells were stained with anti-β-tubulin (green), human serum (red), and Draq5 (blue). B) Multinucleation of infected cells was evaluated. Uninfected, GPIC and L2 infected cells had a percent multinucleation of 27.6 ± 3.6%, 42.6 ± 1.4% and 49.2 ± 6.4%. There was significance of uninfected and GPIC or L2 infected of $p<0.002$, but no significant difference between species. N=3 experiments with at least 600 cells per experiment. C) Percent of mitotic cells that contained more than 2 spindle poles were evaluated. When treated with griseofulvin, uninfected cells had abnormal spindles 52 ± 3%. Cells infected with GPIC or L2 had abnormal spindles 77 ± 10% and 77 ± 5%, respectively. There was significance of uninfected and GPIC or L2 infected of $p<0.02$, but no significant difference between species. N=3 experiments with at least 100 cells per experiment. D) Mitotic index was performed on griseofulvin treated cells. Uninfected, GPIC and L2 infected cells had a mitotic index of 26.2 ±0.6%, 16.8 ± 1.4% and 19.5 ± 5.3%. There was significance of uninfected and GPIC or L2 infected of $p<0.05$, but no significant difference between species. N=3 experiments with at least 1500 cells per experiment

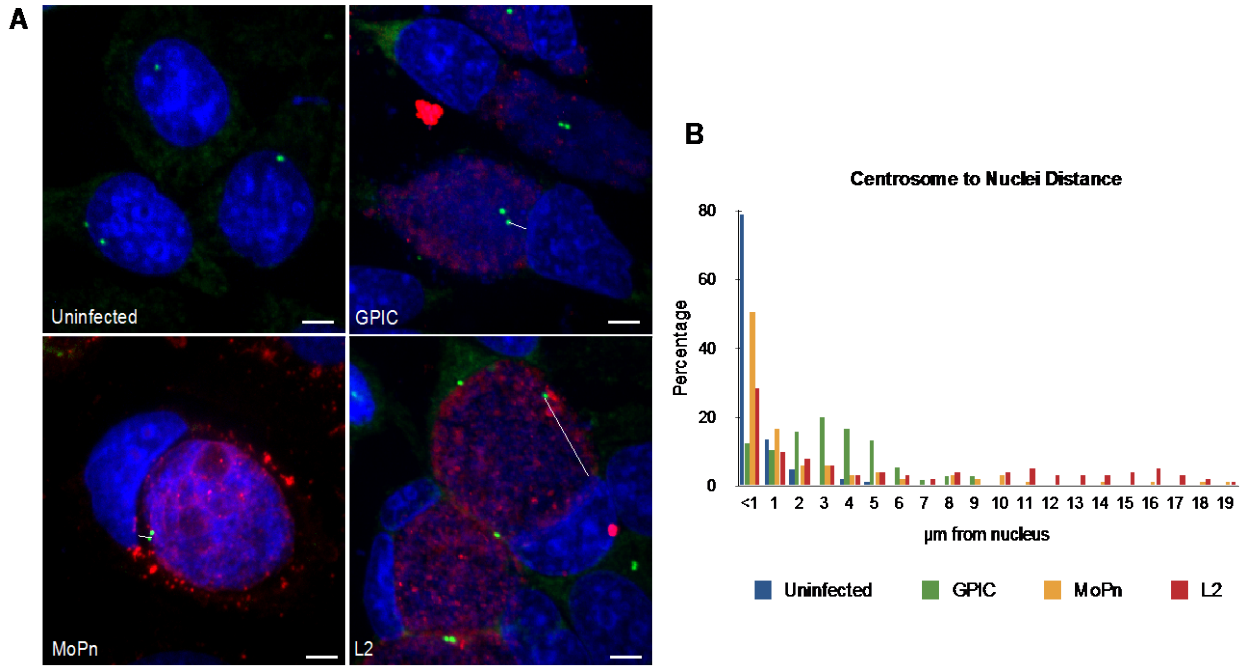

Figure 4-3. Centrosome to nucleus distance. A) HeLa cells were infected with L2, or GPIC for 40 hours. Cells were stained with anti-γ-tubulin (green), human serum (red), and Draq5 (blue). B) The distance between the closest centrosome and the nuclei was measured. Distances are presented in a histogram. The majority of uninfected cells have the centrosome within 1 µm of the nucleus. GPIC and MoPn infected cells have centrosomes shifted away from the nucleus, but mostly remain within 5µm. L2 has a long tail on the histogram, with centrosomes that are up to 19 µm away from the nucleus. There is a significant difference in the mean distance between populations (ANOVA) N=100 cells, per population.

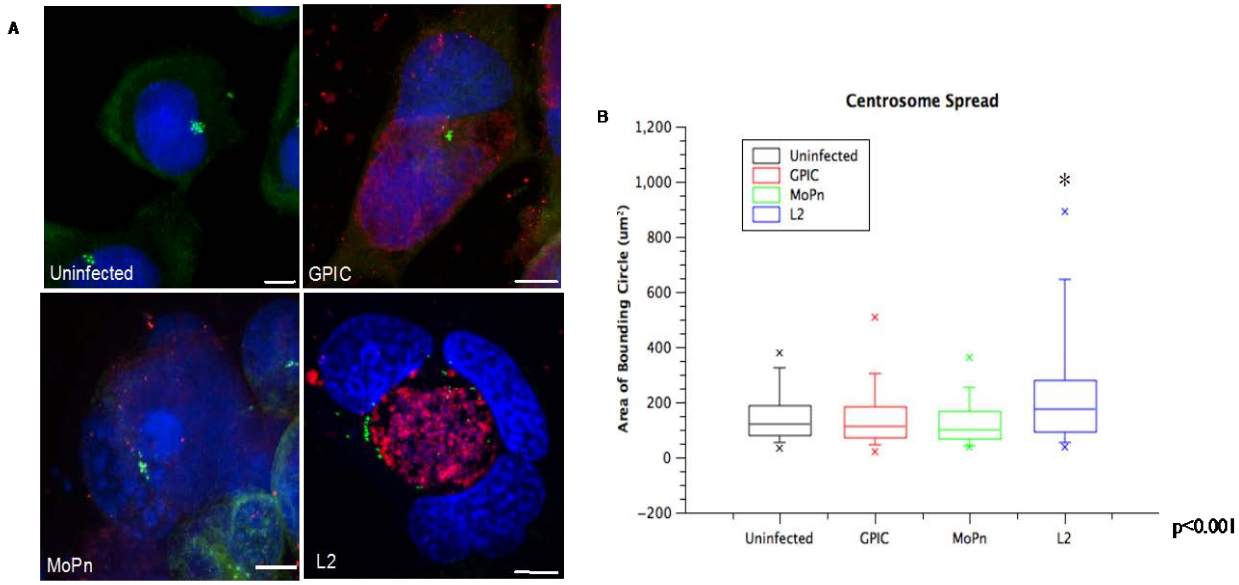

Figure 4-4. Centrosome clustering in neuroblastoma cells. A) Neuroblastoma cells were infected with L2, MoPn or GPIC for 40 hours. Cells were stained with anti-γ-tubulin (green), human serum (red), and Draq5 (blue). B) The centrosome spread was measured with a bounding circle and was graphed with a box and whisker plot. Uninfected cells clustered the centrosomes within 147.6 ± 83.6 μm^2. When infected with GPIC, MoPn or L2 the centrosome where contained within 141.2 ± 89.7 μm, 122.3 ±70.6 μm and 228.8 ±189.4 μm, respectively. There was not a sigificant difference between uninfected and GPIC or MoPn infected cells (ANOVA), but L2 had a significance of $p<0.001$ compared the other species. N=100 cells.

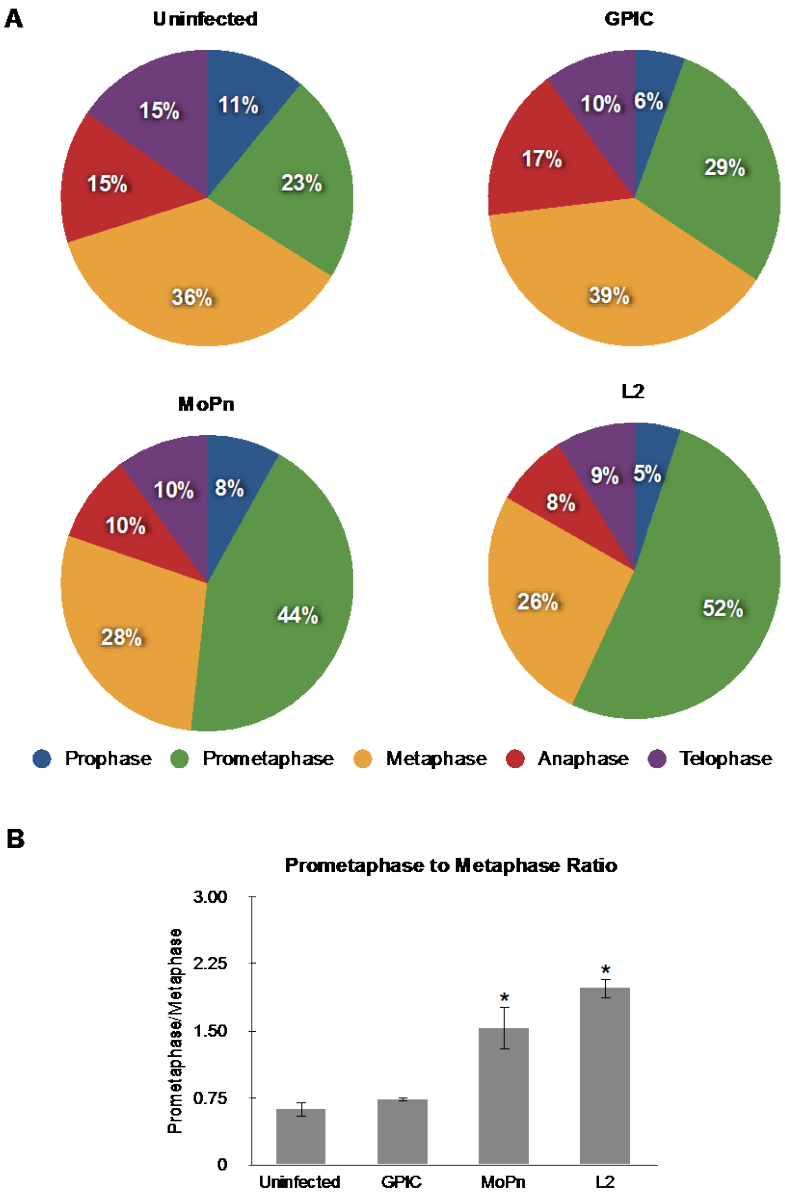

Figure 4-5. Mitosis is disorganized upon infection with L2. HeLa cells were infected with L2, MoPn or GPIC for 40 hours. Cells were stained with anti-β-tubulin (green), human serum (red), and Draq5 (blue). A) The stages of cells in mitosis were analyzed. GPIC infected cells have a similar profile to the stages of mitosis of uninfected cells. Both MoPn and L2 show a shift to predominantly prometaphase, though L2 demonstrates are larger shift. N=3 experiments with 200 cells per experiment. B) The prometaphase to metaphase ratio was evaluated. Uninfected cells had a ratio of 0.6 ± 0.1, while GPIC, MoPn and L2 had a ratio of 0.7, 1.5 ± 0.3 and 2.0 ± 0.1, respectively. The groups had significantly different means (ANOVA). N=3 experiments with 200 cells per experiment.

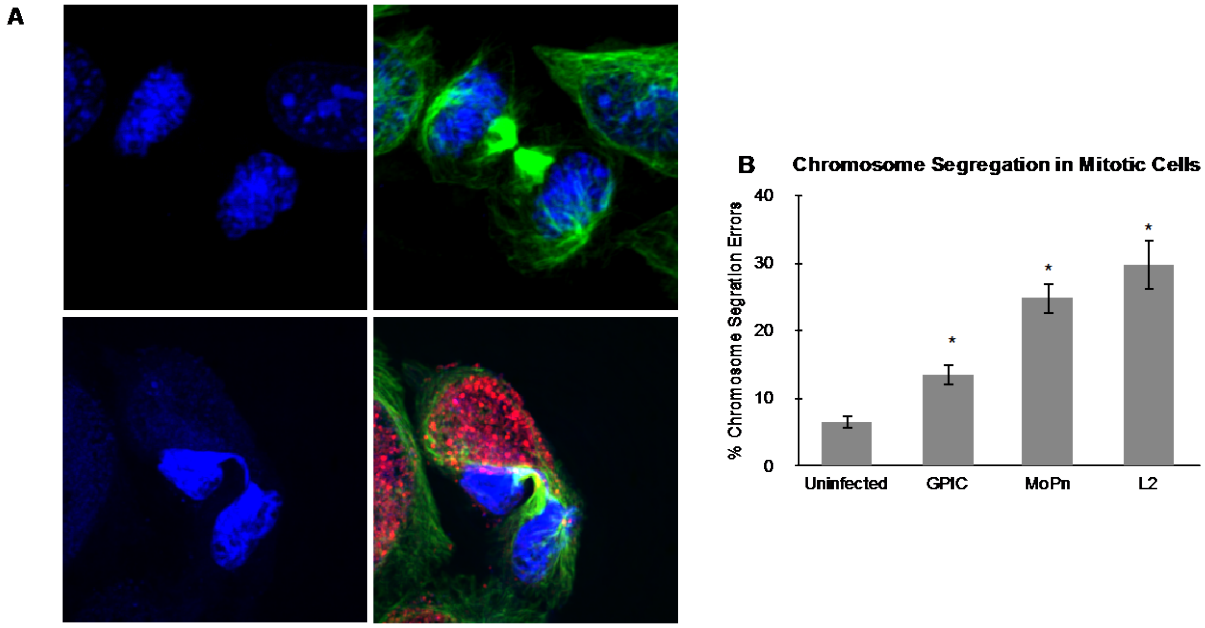

Figure 4-6. DNA segregation errors correlate with multinucleation. A) HeLa cells were infected with L2, MoPn or GPIC for 40 hours. Cells were stained with anti-β-tubulin (green), human serum (red), and Draq5 (blue). B) Cells exiting mitosis were evaluated for DNA bridges and lagging chromosomes. Uninfected cells had a DNA bridging rate of 6.4 ± 1.1%. Upon infection, cells infected with GPIC had a rate of 13.5 ± 1.6%, MoPn had a rate of 24.8 ± 2.5% and L2 had a rate of 29.7 ± 3.8%. The groups had significantly different means (ANOVA). There was a significance of $p > 0.005$ for any infection compared to uninfected. N=3 experiments with 100 cells per experiment.

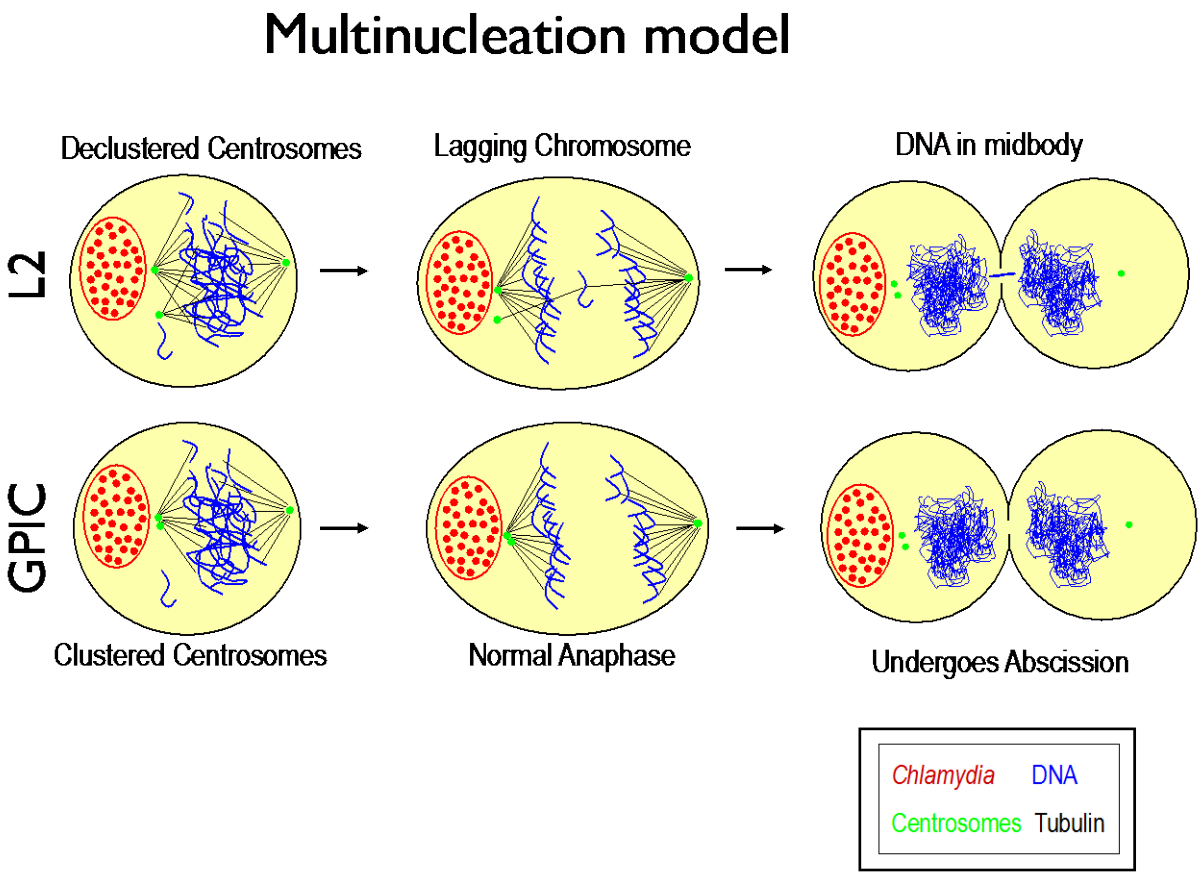

Figure 4-7 Model of differences in multinucleation. Upon infection centrosomes are amplified in host cells. In L2 infected cells, centrosomes are pulled away from the nucleus and dispersed throughout the cell, resulting in declustered centrosome. This leads lagging chromosomes, which when not cleared from the midbody, results in the cell aborting cytokinesis. In GPIC infected cells, centrosome positioning is only disturbed slightly, allowing the centrosomes to cluster during mitosis. This results in a normal mitosis and completion of cytokinesis.

CHAPTER 5
DISCUSSION

Hanahan and Weinberg outlined eight hallmarks of cancer that enable tumor growth and two enabling characteristics that allow hallmark acquisition to be possible. (Hanahan and Weinberg, 2000; 2011). *Chlamydia* infection has been shown to enable two hallmarks in infected host cells: sustaining proliferative signaling and resisting cell death (Jungas et al., 2004; Knowlton et al., 2013). Importantly, *Chlamydia* also contributes to the two enabling characteristics: tumor-promoting inflammation and genome instability. Chlamydial infection promotes a strong inflammatory response that fosters an environment for transformation (Roshick et al., 2006; Rusconi and Greub, 2011). Furthermore, *Chlamydia* can induce disorganized mitosis and multinucleation leading to genomic instability (Knowlton et al., 2011; Sun et al., 2011). Our model suggests that genomic instability due to *Chlamydia* infection contributes to the higher incidence of cervical cancer in women with a prior *C. trachomatis* infection.

Multinucleation of host cells due to a *Chlamydia* infection has been recognized for many years and therefore we aimed to determine the mechanism by which host cells become multinucleated (Horoschak and Moulder, 1978; Bose and Liebhaber, 1979; Greene and Zhong, 2003). We demonstrated multinucleation occurs through cytokinesis failure and ruled out a contribution by cell fusion. In our study, we examined the steps in cytokinesis to determine where cytokinesis failure occurs. Two studies have suggested cytokinesis failure occurs because *Chlamydia* acts as a large bolus of material that causes steric interference, which leads to cytokinesis failure (Campbell et al., 1989; Sun et al., 2011). When we examined the first two steps in cytokinesis we found no change in the cleavage furrow or the percentage of cells that formed midbodies. Furthermore,

multinucleation was not induced by *Coxiella burnetii*, another obligate intracellular bacteria that reside in a large vacuole within the cell. This suggested the failure in cytokinesis was not due to steric interference and multinucleation of the host cell was chlamydial specific. Since steric interference did not account for a large portion of failures in cytokinesis we examined the final step of cytokinesis, abscission. We demonstrated that cells fail extremely late in cytokinesis. Using live cell imaging, we observed differential expression of GFP-bicaudal D1 between the forming daughter cells, suggesting an inhibition of diffusion. This only occurs once the midbody has formed, so therefore cytokinesis fails at abscission. Since the most likely cause of abscission failure is DNA segregation errors, we examined the effect chlamydial infection had on mitosis. We found *C. trachomatis*-infected cells underwent mitosis more rapidly and were able to escape a monastrol block, which suggested chlamydial infection had weakened the SAC. We found that a rapid, disorganized mitosis led to chromosome segregation errors and confirmed that the population of cells that failed cytokinesis was the same population that contained DNA in the midbody of the cell. This evidence leads us to our model of *C. trachomatis*-induced DNA segregation errors during mitosis are the leading cause of cytokinesis failure in infected cells.

We proposed a model in which *Chlamydia*'s ability to override the SAC was due to degradation of cyclin B1 and securin by the protease CPAF. Recently published data demonstrated that degradation observed in western blot analysis was due to enhanced CPAF activity in the sample buffer. When proteins were collected in 8M urea, cyclin B1 was not degraded during the course of the *Chlamydia* infection (Chen et al., 2012). We confirmed these findings by western blot analysis and found cyclin B1 and securin were

not cleaved in detectable levels when lysed in 8M urea (data not shown). We plan to examine CPAF further as the cause of premature mitotic exit because cyclin B1 and securin are not degraded when a CPAF inhibitor is added to the sample buffer, suggesting under certain conditions CPAF can degrade cyclin B1 and securin (Brown et al., 2012). Furthermore, both the cell cycle and developmental cycle are asynchronous, which complicates western blot analysis. Therefore, we propose that a chlamydial protease, that may or may not be CPAF, acts on a different target in the Spindle Assembly Checkpoint pathway. We will further investigate the way *Chlamydia* overrides the SAC with live cell imaging to study the events of a single cell at a time.

Next, we aimed to determine if multinucleation was conserved among divergent *Chlamydia* species. *C. trachomatis* causes amplified centrosomes, declustered centrosomes, premature mitotic exit and multinucleation (Grieshaber et al., 2006; Johnson et al., 2009; Knowlton et al., 2011; Brown et al., 2012). In order to investigate which phenotypes were conserved among species, we compared cytological change in three species of *Chlamydia*. All three species investigated caused shorten mitosis and centrosome amplification, demonstrating that these phenotypes are highly conserved among *Chlamydia*. We found that multinucleation rates and multipolar spindle rates varied among species. Both phenotypes followed the same trend, suggesting that multipolar spindles were the cause of the multinucleation. To test this theory, we forced centrosomes to decluster during infection using griseofulvin. From this, we conclude that shortened mitosis, amplified and declustered centrosomes are all necessary for cytokinesis failure.

We have shown that *Chlamydia* overrides the SAC, which forces the cell to undergo mitosis more rapidly. Mislocalized centrosomes require extra time to form a pseudo-bipolar spindle, which is controlled by the SAC. We found that centrosomes remained near the nucleus and clustered when host cells were infected with GPIC and MoPn, but centrosomes moved away from the nucleus and spread throughout the cell when infected with L2. Declustered centrosomes cause a disorganized mitosis in several ways. The most striking phenotype is multipolar mitosis, but some only undergo a transitory multipolar spindle intermediate before extra centrosomes are clustered into a pseudo-bipolar spindle (Ganem et al., 2009). This transitory state promotes merotelic attachments, causing chromosome segregation errors.

In the future we plan to determine how the chlamydial inclusions from the three species interact with the centrosomes. The differences in inclusion-centrosome interaction would account for the variation in centrosome spread during interphase and the rate of multipolar mitosis. The chlamydial inclusion interacts with the centrosome through dynein, but the specific chlamydial proteins have not been identified (Grieshaber et al., 2003). We plan to identify the chlamydial proteins in the inclusion that interact with the centrosome. Species variation in this unknown protein could account for the differences in centrosome spread.

Next, we plan to determine if specific chromosomes become trapped in the midbody of infected cells, or if trapped chromosomes are random. We will synchronized the cells with a double thymidine block and then perform fluorescence *in situ* hybridization (FISH) on cells exiting mitosis. This experiment will provide new insites the mechanism driving chromosome segregation errors in *Chlamydia*-infected cells.

Finally, our lab will continue studying the mechanism by which chlamydial infection causes premature exit from mitosis and centrosome amplification. Because these two phenotypes are conserved among all species, we hypothesize that one chlamydial effector causes both these phenotypes. The protein complex termed cohesin prevents mitotic exit and centrosome replication. Cohesin forms a ring structure around sister chromosomes and centrosomes, inhibiting sister chromosome and centrosome disengagement (Wittmann et al., 2001; Schöckel et al., 2011). In uninfected cells, the protease separase cleaves cohesin on both chromosomes and centrosomes during mitotic exit. We hypothesize that a chlamydial protease cleaves cohesin prematurely. Preliminary data from our lab suggests that the targeted protein is Ssc1, part of the ring structure of the cohesin complex.

Chlamydial infection causes centrosome amplification during G2 and in this study we demonstrated that *Chlamydia*-infected cells spend more time in G2 than uninfected cells (Johnson et al., 2009). We hypothesize that the elongated G2 phase, paired with a chlamydial protease working as a separase mimic, allows centrioles to prematurely separate and reduplicate. We will explore this hypothesis using live cell imaging and a separase sensor construct provided by Dr. Stemmann (Schöckel et al., 2011). The construct consists of a fusion of four functional domains: a targeting domain, the mCherry fluorescent protein, the Ssc1 cleavage domain, followed by the EGFP protein. The provided construct has H2B as the targeting domain to cause the fusion protein to locate to the chromosomes. We will change this targeting domain to centrin, in order to also visualize centrosome dynamics. Live cell imaging with these constructs will

provide us with further insight into the mechanism of cytokinesis failure. More studies need to be performed to fully understand host cell cytokinesis failure; however, the results presented here provide new insights into *Chlamydia*'s role in multinucleation, centrosome declustering and genomic instability.

LIST OF REFERENCES

Alibek, K., Karatayeva, N., and Bekniyazov, I. (2012). The role of infectious agents in urogenital cancers. Infect. Agents Cancer *7*, 35.

Alzhanov, D.T., Weeks, S.K., Burnett, J.R., and Rockey, D.D. (2009). Cytokinesis is blocked in mammalian cells transfected with Chlamydia trachomatis gene CT223. BMC Microbiol. 9, 2.

Anderhub, S.J., Krämer, A., and Maier, B. (2012). Centrosome amplification in tumorigenesis. Cancer Lett. *322*, 8–17.

Andersen, J.S., Wilkinson, C.J., Mayor, T., Mortensen, P., Nigg, E.A., and Mann, M. (2003). Proteomic characterization of the human centrosome by protein correlation profiling. Nature *426*, 570–574.

Andreassen, P.R., Lohez, O.D., Lacroix, F.B., and Margolis, R.L. (2001). Tetraploid state induces p53-dependent arrest of nontransformed mammalian cells in G1. Mol Biol Cell *12*, 1315–1328.

Anttila, T., Saikku, P., Koskela, P., Bloigu, A., Dillner, J., Ikäheimo, I., Jellum, E., Lehtinen, M., Lenner, P., Hakulinen, T., et al. (2001). Serotypes of Chlamydia trachomatis and risk for development of cervical squamous cell carcinoma. Jama *285*, 47–51.

Baker, D.J., Dawlaty, M.M., Galardy, P., and van Deursen, J.M. (2007). Mitotic regulation of the anaphase-promoting complex. Cell Mol Life Sci *64*, 589–600.

Balsara, Z.R., Misaghi, S., Lafave, J.N., and Starnbach, M.N. (2006). Chlamydia trachomatis infection induces cleavage of the mitotic cyclin B1. Infection and Immunity 74, 5602–5608.

Belland, R., Ojcius, D.M., and Byrne, G.I. (2004). Chlamydia. Nat Rev Microbiol *2*, 530–531.

Benanti, J.A. (2012). Coordination of cell growth and division by the ubiquitin-proteasome system. Seminars in Cell and Developmental Biology *23*, 492–498.

Bose, S.K., and Liebhaber, H. (1979). Deoxyribonucleic acid synthesis, cell cycle progression, and division of Chlamydia-infected HeLa 229 cells. Infection and Immunity *24*, 953–957.

Boveri, T. (2008). Concerning the origin of malignant tumours by Theodor Boveri. Translated and annotated by Henry Harris. J Cell Sci *121 Suppl 1*, 1–84.

Brinkley, B.R. (2001). Managing the centrosome numbers game: from chaos to stability in cancer cell division. Trends Cell Biol *11*, 18–21.

Brinkley, B.R., and Goepfert, T.M. (1998). Supernumerary centrosomes and cancer: Boveri's hypothesis resurrected. Cell Motil. Cytoskeleton *41*, 281–288.

Brown, H.M., Knowlton, A.E., and Grieshaber, S.S. (2012). Chlamydial Infection Induces Host Cytokinesis Failure at Abscission. Cell Microbiol.

Burton, M.J., and Mabey, D.C.W. (2009). The global burden of trachoma: a review. PLoS Negl Trop Dis *3*, e460.

Caballe, A., and Martin-Serrano, J. (2011). ESCRT machinery and cytokinesis: the road to daughter cell separation. Traffic 12, 1318–1326.

Campbell, S., Richmond, S.J., and Yates, P. (1989). The development of Chlamydia trachomatis inclusions within the host eukaryotic cell during interphase and mitosis. J. Gen. Microbiol. *135*, 1153–1165.

Cates, W., and Wasserheit, J.N. (1991). Genital chlamydial infections: epidemiology and reproductive sequelae. Am. J. Obstet. Gynecol. *164*, 1771–1781.

Chan, J.Y. (2011). A clinical overview of centrosome amplification in human cancers. Int. J. Biol. Sci. *7*, 1122–1144.

Chen, A.L., Johnson, K.A., Lee, J.K., Sütterlin, C., and Tan, M. (2012). CPAF: a Chlamydial protease in search of an authentic substrate. PLoS Pathog *8*, e1002842.

Cimini, D., Howell, B., Maddox, P., Khodjakov, A., Degrassi, F., and Salmon, E.D. (2001). Merotelic kinetochore orientation is a major mechanism of aneuploidy in mitotic mammalian tissue cells. J Cell Biol 153, 517–527.

Clémenson, C., and Marsolier-Kergoat, M.C. (2009). ScienceDirect.com - DNA Repair - DNA damage checkpoint inactivation: Adaptation and recovery. DNA Repair.

Clifton, D.R., Dooley, C.A., Grieshaber, S.S., Carabeo, R.A., Fields, K.A., and Hackstadt, T. (2005). Tyrosine phosphorylation of the chlamydial effector protein Tarp is species specific and not required for recruitment of actin. Infection and Immunity 73, 3860–3868.

Clifton, D.R., Fields, K.A., Grieshaber, S.S., Dooley, C.A., Fischer, E.R., Mead, D.J., Carabeo, R.A., and Hackstadt, T. (2004). A chlamydial type III translocated protein is tyrosine-phosphorylated at the site of entry and associated with recruitment of actin. Proc Natl Acad Sci USA *101*, 10166–10171.

de Martel, C., Ferlay, J., Franceschi, S., Vignat, J., Bray, F., Forman, D., and Plummer, M. (2012). Global burden of cancers attributable to infections in 2008: a review and synthetic analysis. Lancet Oncol. *13*, 607–615.

Dehoux, P., Flores, R., Dauga, C., Zhong, G., and Subtil, A. (2011). Multi-genome identification and characterization of chlamydiae-specific type III secretion substrates: the Inc proteins. BMC Genomics *12*, 109.

Dong, F., Pirbhai, M., Zhong, Y., and Zhong, G. (2004). Cleavage-dependent activation of a chlamydia-secreted protease. Mol Microbiol *52*, 1487–1494.

Duelli, D., and Lazebnik, Y. (2007). Cell-to-cell fusion as a link between viruses and cancer. Nat Rev Cancer. 7, 968-976.

Eggert, U.S., Mitchison, T.J., and Field, C.M. (2006). Animal cytokinesis: from parts list to mechanisms. Annu. Rev. Biochem. *75*, 543–566.

Ferguson, R.L., and Maller, J.L. (2010). Centrosomal localization of cyclin E-Cdk2 is required for initiation of DNA synthesis. Curr Biol *20*, 856–860.

Fields, K.A., and Hackstadt, T. (2002). The chlamydial inclusion: escape from the endocytic pathway. Annu Rev Cell Dev Biol *18*, 221–245.

Friis, R.R. (1972). Interaction of L cells and Chlamydia psittaci: entry of the parasite and host responses to its development. J Bacteriol *110*, 706–721.

Fujiwara, T., Bandi, M., Nitta, M., Ivanova, E.V., Bronson, R.T., and Pellman, D. (2005). Cytokinesis failure generating tetraploids promotes tumorigenesis in p53-null cells. Nature *437*, 1043–1047.

Fukasawa, K. (2007). Oncogenes and tumour suppressors take on centrosomes. Nat Rev Cancer *7*, 911–924.

Ganem, N.J., and Pellman, D. (2007). Limiting the proliferation of polyploid cells. Cell *131*, 437–440.

Ganem, N.J., and Pellman, D. (2012). Linking abnormal mitosis to the acquisition of DNA damage. J Cell Biol *199*, 871–881.

Ganem, N.J., Godinho, S.A., and Pellman, D. (2009). A mechanism linking extra centrosomes to chromosomal instability. Nature *460*, 278–282.

Gavet, O., and Pines, J. (2010). Progressive activation of CyclinB1-Cdk1 coordinates entry to mitosis. Dev Cell *18*, 533–543.

Glotzer, M. (2001). Animal cell cytokinesis. Annu Rev Cell Dev Biol *17*, 351–386.

Glotzer, M. (2005). The Molecular Requirements for Cytokinesis. Science *307*, 1735–1739.

Gordon, D.J., Resio, B., and Pellman, D. (2012). Causes and consequences of aneuploidy in cancer. Nat. Rev. Genet. 13, 189–203.

Gould, R.R., and Borisy, G.G. (1977). The pericentriolar material in Chinese hamster ovary cells nucleates microtubule formation. J Cell Biol *73*, 601–615.

Greene, W., and Zhong, G. (2003). Inhibition of host cell cytokinesis by Chlamydia trachomatis infection. J Infect *47*, 45–51.

Grieshaber, S.S., Grieshaber, N.A., and Hackstadt, T. (2003). Chlamydia trachomatis uses host cell dynein to traffic to the microtubule-organizing center in a p50 dynamitin-independent process. J Cell Sci *116*, 3793–3802.

Grieshaber, S.S., Grieshaber, N.A., Miller, N., and Hackstadt, T. (2006). Chlamydia trachomatis causes centrosomal defects resulting in chromosomal segregation abnormalities. Traffic *7*, 940–949.

Hackstadt, T., Rockey, D.D., Heinzen, R.A., and Scidmore, M.A. (1996). Chlamydia trachomatis interrupts an exocytic pathway to acquire endogenously synthesized sphingomyelin in transit from the Golgi apparatus to the plasma membrane. Embo J 15, 964–977.

Hackstadt, T., Scidmore, M.A., and Rockey, D.D. (1995). Lipid metabolism in Chlamydia trachomatis-infected cells: directed trafficking of Golgi-derived sphingolipids to the chlamydial inclusion. Proc Natl Acad Sci USA *92*, 4877–4881.
Hanahan, D., and Weinberg, R.A. (2000). The hallmarks of cancer. Cell *100*, 57–70.

Hanahan, D., and Weinberg, R.A. (2011). Hallmarks of cancer: the next generation. Cell *144*, 646–674.

Hartwell, L.H., and Weinert, T.A. (1989). Checkpoints: controls that ensure the order of cell cycle events. Science *246*, 629–634.

Heinzen, R.A., Hackstadt, T., Samuel, J.E. (1999). Developmental biology of *Coxiella burnettii*. Trends in Microbiology 7, 149–154.

Heinzen, R.A., Scidmore, M.A., Rockey, D.D., Hackstadt, T. (1996). Differential interaction with endocytic and exocytic pathways distinguish parasitophorous vacuoles of *Coxiella burnetii* and *Chlamydia trachomatis*. Infect. Immun. 64, 796–809.

Horoschak, K.D., and Moulder, J.W. (1978). Division of single host cells after infection with chlamydiae. Infection and Immunity *19*, 281–286.

Hu, V.H., Harding-Esch, E.M., Burton, M.J., Bailey, R.L., Kadimpeul, J., and Mabey, D.C.W. (2010). Epidemiology and control of trachoma: systematic review. Trop Med Int Health 15, 673-691.

Huang, Z., Feng, Y., Chen, D., Wu, X., Huang, S., Wang, X., Xiao, X., Li, W., Huang, N., Gu, L., et al. (2008). Structural basis for activation and inhibition of the secreted chlamydia protease CPAF. Cell Host Microbe 4, 529–542.

Iliffe-Lee, E.R., and McClarty, G. (2000). Regulation of carbon metabolism in Chlamydia trachomatis. Mol Microbiol *38*, 20–30.

Jirawatnotai, S., Hu, Y., Livingston, D.M., and Sicinski, P. (2012). Proteomic identification of a direct role for cyclin d1 in DNA damage repair. Cancer Res. *72*, 4289–4293.

Johnson, K.A., Tan, M., and Sütterlin, C. (2009). Centrosome abnormalities during a Chlamydia trachomatis infection are caused by dysregulation of the normal duplication pathway. Cell Microbiol *11*, 1064–1073.

Jorgensen, I., Bednar, M.M., Amin, V., Davis, B.K., Ting, J.P.Y., McCafferty, D.G., and Valdivia, R.H. (2011). The Chlamydia Protease CPAF Regulates Host and Bacterial Proteins to Maintain Pathogen Vacuole Integrity and Promote Virulence. Cell Host Microbe *10*, 21–32.

Jungas, T., Verbeke, P., Darville, T., and Ojcius, D.M. (2004). Cell death, BAX activation, and HMGB1 release during infection with Chlamydia. Microbes and Infection *6*, 1145–1155.

Kapoor, T.M., Mitchison, T.J. (2001). Eg5 is static in bipolar spindles relative to tubulin: evidence for a static spindle matrix. J Cell Biol 154, 1125–1133.

Kim, S., Yu, H. (2011). Mutual regulation between the spindle checkpoint and APC/C. Seminars in Cell and Developmental Biology 22, 551-558.

Kevin Hybiske, R.S.S. (2007) Mechanisms of host cell exit by the intraceullular bacterium *Chlamydia.* Proc Natl Acad Sci U.S.A 104, 11430-11435.

King R.W. (2008). When 2+2=5: the origins and fates of aneuploid and tetraploid cells. Biochim. Biophys. Acta 1786, 4–14.

Kiviat, N.B., Paavonen, J.A., Brockway, J., Critchlow, C.W., Brunham, R.C., Stevens, C.E., Stamm, W.E., Kuo, C.C., DeRouen, T., and Holmes, K.K. (1985). Cytologic manifestations of cervical and vaginal infections. I. Epithelial and inflammatory cellular changes. JAMA : The Journal Of The American Medical Association 253, 989-96.

Knowlton, A.E., Brown, H.M., Richards, T.S., Andreolas, L.A., Patel, R.K., and Grieshaber, S.S. (2011). Chlamydia trachomatis infection causes mitotic spindle pole defects independently from its effects on centrosome amplification. Traffic.

Knowlton, A.E., Fowler, L.J., Patel, R.K., Wallet, S.M., and Grieshaber, S.S. (2013). Chlamydia Induces Anchorage Independence in 3T3 Cells and Detrimental Cytological Defects in an Infection Model. PLoS ONE *8*, e54022.

Korzeniewski, N., Spardy, N., Duensing, A., Duensing, S. (2011). Genomic instability and cancer: lessons learned from human papillomaviruses. Cancer Lett. 305, 113–122.

Koskela, P., Anttila, T., Bjørge, T., Brunsvig, A., Dillner, J., Hakama, M., Hakulinen, T., Jellum, E., Lehtinen, M., Lenner, P., et al. (2000). Chlamydia trachomatis infection as a risk factor for invasive cervical cancer. Int J Cancer *85*, 35–39.

Kuriyama, R., and Borisy, G.G. (1981). Centriole cycle in Chinese hamster ovary cells as determined by whole-mount electron microscopy. J Cell Biol *91*, 814–821.

Kwon, M., Godinho, S.A., Chandhok, N.S., Ganem, N.J., Azioune, A., Thery, M., and Pellman, D. (2008). Mechanisms to suppress multipolar divisions in cancer cells with extra centrosomes. Genes Dev *22*, 2189–2203.

Liu, B., Hong, S., Tang, Z., Yu, H., Giam, C.Z., (2005). HTLV-I Tax directly binds the Cdc20-associated anaphase-promoting complex and activates it ahead of schedule. Proc. Natl. Acad. Sci. U.S.A. 102, 63–68.

Lohez, O.D., Reynaud, C., Borel, R., Andreassen P.R., Marglois, R.L. (2003). Arrest of mammalian fibroblasts in G1 in response to actin inhibition is dependent on retinoblastoma pocket proteins but not on p53. J Cell BIol 161, 67-77.

Madeleine, M.M., Anttila, T., Schwartz, S.M., Saikku, P., Leinonen, M., Carter, J.J., Wurscher, M., Johnson, L.G., Galloway, D.A., and Daling, J.R. (2007). Risk of cervical cancer associated with Chlamydia trachomatis antibodies by histology, HPV type and HPV cofactors. Int J Cancer *120*, 650–655.

Marangos, P., and Carroll, J. (2008). Securin regulates entry into M-phase by modulating the stability of cyclin B. Nat Cell Biol 10, 445–451.

Matanis, T., Akhmanova, A., Wulf, P., Del Nery, E., Weide, T., Stepanova, T., Galjart, N., et al. (2002). Bicaudal-D regulates COPI-independent Golgi-ER transport by recruiting the dynein-dynactin motor complex. Nat. Cell Biol. 4, 986–992.

Matsumoto, K., Yasugi, T., Oki, A., Hoshiai, H., Taketani, Y., Kawana, T., and Yoshikawa, H. (2003). Are smoking and chlamydial infection risk factors for CIN? Different results after adjustment for HPV DNA and antibodies. Br. J. Cancer *89*, 831–833.

McLaughlin-Drubin, M.E., Münger, K. (2009). The human papillomavirus E7 oncoprotein. Virology 384: 335–344.

McLean, J.R., Chaix, D., Ohi, M.D., Gould, K.L. (2011). State of the APC/C: organization, function, and structure. Crit. Rev. Biochem. Mol. Biol. 46, 118–136.

Mendoza, M., Norden, C., Durrer, K., Rauter, H., Uhlmann, F., and Barral, Y. (2009). A mechanism for chromosome segregation sensing by the NoCut checkpoint. Nat Cell Biol *11*, 477–483.

Menoyo, S., Ricco, N., Bru, S., Hernández-Ortega, S., Escoté, X., Aldea, M., and Clotet, J. (2013). Phosphate-activated cyclin-dependent kinase stabilizes g1 cyclin to trigger cell cycle entry. Mol. Cell. Biol. *33*, 1273–1284.

Moorhead, A.R., Rzomp, K.A., and Scidmore, M.A. (2007). The Rab6 effector Bicaudal D1 associates with Chlamydia trachomatis inclusions in a biovar-specific manner. Infection and Immunity 75, 781–791.

Moulder, J.W. (1991). Interaction of chlamydiae and host cells in vitro. Microbiol Rev *55*, 143–190.

Nigg, E.A. (2002). Centrosome aberrations: cause or consequence of cancer progression? Nat Rev Cancer *2*, 815–825.

Norden, C., Mendoza, M., Dobbelaere, J., Kotwaliwale, C.V., Biggins, S., and Barral, Y. (2006). The NoCut pathway links completion of cytokinesis to spindle midzone function to prevent chromosome breakage. Cell *125*, 85–98.

Normand, G., King, R.W. (2010). Understanding cytokinesis failure. Adv Exp Med Biol 676, 27-55.

Paschen, S.A., Christian, J.G., Vier, J., Schmidt, F., Walch, A., Ojcius, D.M., and Häcker, G. (2008). Cytopathicity of Chlamydia is largely reproduced by expression of a single chlamydial protease. J Cell Biol *182*, 117–127.

Peters, J.-M. (2006). The anaphase promoting complex/cyclosome: a machine designed to destroy. Nat Rev Mol Cell Biol *7*, 644–656.

Piel, M., Meyer, P., Khodjakov, A., Rieder, C.L., and Bornens, M. (2000). The respective contributions of the mother and daughter centrioles to centrosome activity and behavior in vertebrate cells. J Cell Biol *149*, 317–330.

Pihan, G.A., Purohit, A., Wallace, J., Knecht, H., Woda, B., Quesenberry, P., and Doxsey, S.J. (1998). Centrosome defects and genetic instability in malignant tumors. Cancer Res. *58*, 3974–3985.

Pines, J. (2011). Cubism and the cell cycle: the many faces of the APC/C. Nat Rev Mol Cell Biol.

Pisani, P., Parkin, D.M., Muñoz, N., and Ferlay, J. (1997). Cancer and infection: estimates of the attributable fraction in 1990. Cancer Epidemiol Biomarkers Prev *6*, 387–400.

Quintyne, N.J., Reing, J.E., Hoffelder, D.R., Gollin, S.M., and Saunders, W.S. (2005). Spindle multipolarity is prevented by centrosomal clustering. Science *307*, 127–129.

Ramos, J.G., Varayoud, J., Bosquiazzo, V.L., Luque, E.H., Muñoz-de-Toro, M. (2002). Cellular turnover in the rat uterine cervix and its relationship to estrogen and progesterone receptor dynamics. Biol Reprod 67, 735–742.

Read, T.D., Brunham, R.C., Shen, C., Gill, S.R., Heidelberg, J.F., White, O., Hickey, E.K., Peterson, J., Utterback, T., Berry, K., et al. (2000). Genome sequences of Chlamydia trachomatis MoPn and Chlamydia pneumoniae AR39. Nucleic Acids Res. *28*, 1397–1406.

Read, T.D., Myers, G.S.A., Brunham, R.C., Nelson, W.C., Paulsen, I.T., Heidelberg, J., Holtzapple, E., Khouri, H., Federova, N.B., Carty, H.A., et al. (2003). Genome sequence of Chlamydophila caviae (Chlamydia psittaci GPIC): examining the role of niche-specific genes in the evolution of the Chlamydiaceae. Nucleic Acids Res. *31*, 2134–2147.

Ring, D., Hubble, R., and Kirschner, M. (1982). Mitosis in a cell with multiple centrioles. J Cell Biol *94*, 549–556.

Roset Bahmanyar, E., Paavonen, J., Naud, P., Salmerón, J., Chow, S.-N., Apter, D., Kitchener, H., Castellsagué, X., Teixeira, J.C., Skinner, S.R., et al. (2012). Prevalence and risk factors for cervical HPV infection and abnormalities in young adult women at enrolment in the multinational PATRICIA trial. Gynecol. Oncol. *127*, 440–450.

Roshick, C., Wood, H., Caldwell, H.D., and McClarty, G. (2006). Comparison of gamma interferon-mediated antichlamydial defense mechanisms in human and mouse cells. Infection and Immunity *74*, 225–238.

Rusconi, B., and Greub, G. (2011). Chlamydiales and the innate immune response: friend or foe? FEMS Immunol Med Microbiol *61*, 231–244.

Saka, H.A., and Valdivia, R.H. (2010). Acquisition of nutrients by Chlamydiae: unique challenges of living in an intracellular compartment. Curr Opin Microbiol *13*, 4–10.

Sakaue-Sawano, A., Kurokawa, H., Morimura, T., Hanyu, A., Hama, H. Osawa, H., et al. (2008) Visualizing spatiotemporal dynamics of multicellular cell-cycle progression. Cell 132, 487–498.

Samaras, V., Rafailidis, P.I., Mourtzoukou, E.G., Peppas, G., and Falagas, M.E. (2010). Chronic bacterial and parasitic infections and cancer: a review. J Infect Dev Ctries 4, 267–281–15.

Saunders, W. (2005). Centrosomal amplification and spindle multipolarity in cancer cells. Semin. Cancer Biol. *15*, 25–32.

Schmidt, K., and Nichols, B.J. (2004). A barrier to lateral diffusion in the cleavage furrow of dividing mammalian cells. Curr Biol *14*, 1002–1006.

Schöckel, L., Möckel, M., Mayer, B., Boos, D., and Stemmann, O. (2011). Cleavage of cohesin rings coordinates the separation of centrioles and chromatids. Nat Cell Biol *13*, 966–972.

Shaw, A.C., Vandahl, B.B., Larsen, M.R., Roepstorff, P., Gevaert, K., Vandekerckhove, J., Christiansen, G., and Birkelund, S. (2002). Characterization of a secreted Chlamydia protease. Cell Microbiol *4*, 411–424.

Smith, J.S., Bosetti, C., Muñoz, N., Herrero, R., Bosch, F.X., Eluf-Neto, J., Meijer, C.J.L.M., Van Den Brule, A.J.C., Franceschi, S., Peeling, R.W., et al. (2004). Chlamydia trachomatis and invasive cervical cancer: a pooled analysis of the IARC multicentric case-control study. Int J Cancer *111*, 431–439.

Smith, J.S., Muñoz, N., Herrero, R., Eluf-Neto, J., Ngelangel, C., Franceschi, S., Bosch, F.X., Walboomers, J.M.M., and Peeling, R.W. (2002). Evidence for Chlamydia trachomatis as a human papillomavirus cofactor in the etiology of invasive cervical cancer in Brazil and the Philippines. J. Infect. Dis. *185*, 324–331.

Steigemann, P., and Gerlich, D.W. (2009a). An evolutionary conserved checkpoint controls abscission timing. Cell Cycle *8*, 1814–1815.

Steigemann, P., and Gerlich, D.W. (2009b). Cytokinetic abscission: cellular dynamics at the midbody. Trends Cell Biol *19*, 606–616.

Steigemann, P., Wurzenberger, C., Schmitz, M.H.A., Held, M., Guizetti, J., Maar, S., and Gerlich, D.W. (2009). Aurora B-mediated abscission checkpoint protects against tetraploidization. Cell 136, 473–484.

Stephens, R.S., Kalman, S., Lammel, C., Fan, J., Marathe, R., Aravind, L., Mitchell, W., Olinger, L., Tatusov, R.L., Zhao, Q., et al. (1998). Genome sequence of an obligate intracellular pathogen of humans: Chlamydia trachomatis. Science *282*, 754–759.

Sun, H.S., Wilde, A., and Harrison, R.E. (2011). Chlamydia trachomatis inclusions induce asymmetric cleavage furrow formation and ingression failure in host cells. Mol. Cell. Biol. *31*, 5011–5022.

Swanson, J., Eschenbach, D.A., Alexander, E.R., and Holmes, K.K. (1975). Light and electron microscopic study of Chlamydia trachomatis infection of the uterine cervix. J. Infect. Dis. *131*, 678–687.

Todd, W.J., Caldwell, H.D. (1985). The interaction of *Chlamydia trachomatis* with host cells: ultrastructural studies of the mechanism of release of a biovar II strain from HeLa 229 cells. J Infect Dis *151*, 1037-1044.

Thompson, S.L., Bakhoum, S.F., Compton, D.A. (2010). Mechanisms of chromosomal instability. Curr Biol *20*, 285-95.

Uetake, Y., and Sluder, G. (2004). Cell cycle progression after cleavage failure: mammalian somatic cells do not possess a "tetraploidy checkpoint". J Cell Biol *165*, 609–615.

Uhlmann, F., Lottspeich, F., and Nasmyth, K. (1999). Sister-chromatid separation at anaphase onset is promoted by cleavage of the cohesin subunit Scc1. Nature *400*, 37–42.

van Leuken, R., Clijsters, L., and Wolthuis, R. (2008). To cell cycle, swing the APC/C. Biochim Biophys Acta 1786, 49–59.

Vogel, J.M., Stearns, T., Rieder, C.L., and Palazzo, R.E. (1997). Centrosomes isolated from Spisula solidissima oocytes contain rings and an unusual stoichiometric ratio of alpha/beta tubulin. J Cell Biol *137*, 193–202.

Wallin, K.-L., Wiklund, F., Luostarinen, T., Angström, T., Anttila, T., Bergman, F., Hallmans, G., Ikäheimo, I., Koskela, P., Lehtinen, M., et al. (2002). A population-based prospective study of Chlamydia trachomatis infection and cervical carcinoma. Int J Cancer *101*, 371–374.

Wandke, C., Barisic, M., Sigl, R., Rauch, V., Wolf, F., Amaro, A.C., Tan, C.H., Pereira, A.J., Kutay, U., Maiato, H., et al. (2012). Human chromokinesins promote chromosome congression and spindle microtubule dynamics during mitosis. J Cell Biol *198*, 847–863.

Weihua, Z., Lin, Q., Ramoth, A.J., Fan, D., and Fidler, I.J. (2011). Formation of solid tumors by a single multinucleated cancer cell. Cancer *117*, 4092–4099.

Wheelhouse, N., and Longbottom, D. (2012). Endemic and emerging chlamydial infections of animals and their zoonotic implications. Transbound Emerg Dis *59*, 283–291.

WHO (2001). Global Prevalence and Incidence of Selected Curable Sexually Transmitted Infections: Overview and Estimates. World Health Organizaion, Geneva (2001). 1-50

Wittmann, T., Hyman, A., and Desai, A. (2001). The spindle: a dynamic assembly of microtubules and motors. Nat Cell Biol.

Zhong, G. (2011). Chlamydia trachomatis secretion of proteases for manipulating host signaling pathways. Front Microbiol *2*, 14.

Zhong, G., Fan, P., Ji, H., Dong, F., and Huang, Y. (2001). Identification of a chlamydial protease-like activity factor responsible for the degradation of host transcription factors. J Exp Med *193*, 935–942.

Zyss, D., and Gergely, F. (2009). Centrosome function in cancer: guilty or innocent? Trends Cell Biol *19*, 334–346.

BIOGRAPHICAL SKETCH

Heather Brown was born in Athens, GA, but moved to Penn Yan, NY to complete primary and secondary school. Heather had the opportunity to spend time in her uncle's cytomegalovirus lab, where her love of confocal microscopes started. She then attended University of Rochester where she explored all the different majors in biology, while working in a physiology lab, before settling on Microbiology and Immunology. She was accepted into a summer internship at Whitney Laboratory for Marine Bioscience the summer before senior year. This strengthened her resolve to get her Ph.D. After graduating college, she was admitted into the Interdisplinary Program in Biomedical Sciences at University of Florida. Heather Brown performed her graduate research studies under the supervision of Dr. Scott Grieshaber on the pathogenesis of *Chlamydia*. After obtaining her Ph.D. Heather hopes to have a career in the basic biology of cancer.